

<https://doi.org/10.14379/iodp.proc.365.101.2017>

Expedition 365 summary¹

 Check for updates

A. Kopf, D. Saffer, S. Toczko, E. Araki, S. Carr, T. Kimura, C. Kinoshita, R. Kobayashi, Y. Machida, A. Rösner, and L.M. Wallace with contributions by S. Chiyonobu, K. Kanagawa, T. Kanamatsu, G. Kimura, and M.B. Underwood²

Keywords: International Ocean Discovery Program, IODP, *Chikyu*, Expedition 365, Site C0010, Nankai Trough, Nankai Trough Seismogenic Zone Experiment, NanTroSEIZE, long-term borehole monitoring system, LTBMS, CORK, Mie-ken Nanto-oki earthquake, megasplay fault, Dense Oceanfloor Network System for Earthquakes and Tsunamis, DONET, GeniusPlug, Flow-through Osmo Colonization System, FLOCS, Kumano fore-arc basin, OsmoSampler, borehole observatory

Abstract

The Nankai Trough Seismogenic Zone Experiment (NanTroSEIZE) is a coordinated, multiexpedition International Ocean Discovery Program (IODP) drilling project designed to investigate fault mechanics and seismogenesis along subduction megathrusts through direct sampling, in situ measurements, and long-term monitoring in conjunction with allied laboratory and numerical modeling studies. The fundamental scientific objectives of the NanTroSEIZE drilling project include characterizing the nature of fault slip and strain accumulation, fault and wall rock composition, fault architecture, and state variables throughout the active plate boundary system. IODP Expedition 365 is part of NanTroSEIZE Stage 3, with the following primary objectives:

1. Retrieval of a temporary observatory at Site C0010 that began monitoring temperature and pore pressure within the major splay thrust fault (termed the “megasplay”) at 400 meters below seafloor in November 2010.
2. Deployment of a complex long-term borehole monitoring system (LTBMS) designed to be connected to the Dense Oceanfloor Network System for Earthquakes and Tsunamis (DONET) seafloor cabled observatory network postexpedition.

The LTBMS incorporates multilevel pore pressure sensing, a volumetric strainmeter, tiltmeter, geophone, broadband seismometer, accelerometer, and thermistor string. Together with an existing observatory at Integrated Ocean Drilling Program Site C0002 and a planned future installation near the trench, the Site C0010 observatory allows monitoring within and above regions of contrasting behavior of the megasplay fault and the plate boundary as a whole. These include a site above the updip edge of the locked zone (Site

C0002), a shallow site in the megasplay fault zone and its footwall (Site C0010), and a site at the tip of the accretionary prism (possible future installation at Integrated Ocean Drilling Program Site C0006). Together, this suite of observatories has the potential to capture deformation spanning a wide range of timescales (e.g., seismic and microseismic activity, slow slip, and interseismic strain accumulation) across a transect from near-trench to the seismogenic zone. Site C0010 is located 3.5 km along strike to the southwest of Integrated Ocean Drilling Program Site C0004. The site was drilled and cased during Integrated Ocean Drilling Program Expedition 319, with casing screens spanning a ~20 m interval that includes the megasplay fault, and suspended with a temporary instrument package (a “SmartPlug”), which included pressure and temperature sensors. During Integrated Ocean Drilling Program Expedition 332 in late 2010, the instrument package was replaced with an upgraded sensor package (the “GeniusPlug”), which included a set of geochemical and biological experiments in addition to pressure and temperature sensors.

Expedition 365 achieved its primary scientific and operational objectives, including recovery of the GeniusPlug with a >5 y record of pressure and temperature conditions within the shallow megasplay fault zone, geochemical samples, and its in situ microbial colonization experiment; and installation of the LTBMS. The pressure records from the GeniusPlug include high-quality records of formation and seafloor responses to multiple fault slip events, including the 11 March 2011 Tohoku M9 and 1 April 2016 Mie-ken Nanto-oki M6 earthquakes. The geochemical sampling coils yielded in situ pore fluids from the splay fault zone, and microorganisms were successfully cultivated from the colonization unit. The complex sensor array, in combination with the multilevel hole completion, is one of the most ambitious and sophisticated observatory installations in

¹ Kopf, A., Saffer, D., Toczko, S., Araki, E., Carr, S., Kimura, T., Kinoshita, C., Kobayashi, R., Machida, Y., Rösner, A., and Wallace, L.M., 2017. Expedition 365 summary. With contributions by S. Chiyonobu, K. Kanagawa, T. Kanamatsu, G. Kimura, and M.B. Underwood. In Saffer, D., Kopf, A., Toczko, S., and the Expedition 365 Scientists, *NanTroSEIZE Stage 3: Shallow Megasplay Long-Term Borehole Monitoring System*. Proceedings of the International Ocean Discovery Program, 365: College Station, TX (International Ocean Discovery Program). <https://doi.org/10.14379/iodp.proc.365.101.2017>

² **Expedition 365 Scientists' addresses.**

MS 365-101: Published 5 August 2017

This work is distributed under the [Creative Commons Attribution 4.0 International \(CC BY 4.0\) license](#). 

Contents

- 1 Abstract
- 2 Introduction
- 2 Background
- 5 Scientific objectives and operational strategy
- 8 Operations
- 10 Principal results
- 15 Preliminary scientific assessment
- 16 References

scientific ocean drilling (similar to that in Hole C0002G, deployed in 2010). Overall, the installation went smoothly, efficiently, and ahead of schedule. The extra time afforded by the efficient observatory deployment was used for coring in Holes C0010B–C0010E. Despite challenging hole conditions, the depth interval corresponding to the screened casing across the megasplay fault was successfully sampled in Hole C0010C, and the footwall of the megasplay was sampled in Hole C0010E, with >50% recovery for both zones.

In the hanging wall of the megasplay fault (Holes C0010C and C0010D), we recovered indurated silty clay with occasional ash layers and sedimentary breccias. Mudstones show different degrees of deformation spanning from occasional fractures to intervals of densely fractured scaly claystones of up to >10 cm thickness. Sparse faulting with low displacement (usually <2 cm) is seen in core and exhibits primarily normal and, rarely, reversed sense of slip. When present, ash was entrained along fractures and faults. In Hole C0010E, the footwall to the megasplay fault was recovered. Sediments are horizontally to gently dipping and mainly comprise silt of olive-gray color. The hanging wall sediments recovered in Holes C0010C–C0010D range in age from 3.79 to 5.59 Ma and have been thrust over the younger footwall sediments in Hole C0010E, ranging in age from 1.56 to 1.67 Ma. The deposits of the underthrust sediment prism are less indurated than the hanging wall mudstones and show lamination on a centimeter scale. The material is less intensely deformed than the mudstones, and apart from occasional fracturation (some of it being drilling disturbance), evidence of structural features is absent.

Introduction

Subduction zones account for 90% of global seismic moment release and generate damaging earthquakes and tsunamis with potentially disastrous effects on heavily populated coastal areas (e.g., Lay et al., 2005; Moreno et al., 2010; Simons et al., 2011). Understanding the processes that govern the strength, nature, and distribution of slip along these plate boundary fault systems is a crucial step toward evaluating earthquake and tsunami hazards. More generally, characterizing fault slip behavior and mechanical state at all plate boundary types through direct sampling, near-field geophysical observations, measurement of in situ conditions, and shore-based laboratory experiments is a fundamental and societally relevant goal of modern earth science. To this end, several recent and ongoing drilling programs have targeted portions of active plate boundary faults that have either slipped coseismically during large earthquakes or have nucleated smaller events. These efforts include the San Andreas Fault Observatory at Depth (Hickman et al., 2004), the Taiwan-Chelungpu Drilling Project (Ma, 2005), and Integrated Ocean Drilling Program drilling in the Nankai Trough (Nankai Trough Seismogenic Zone Experiment [NanTroSEIZE]; Tobin and Kinoshita, 2006a, 2006b) and in the high-slip region of the March 2011 Tohoku earthquake (Japan Trench Fast Drilling Project; Expedition 343/343T Scientists, 2013).

Background

Geological setting

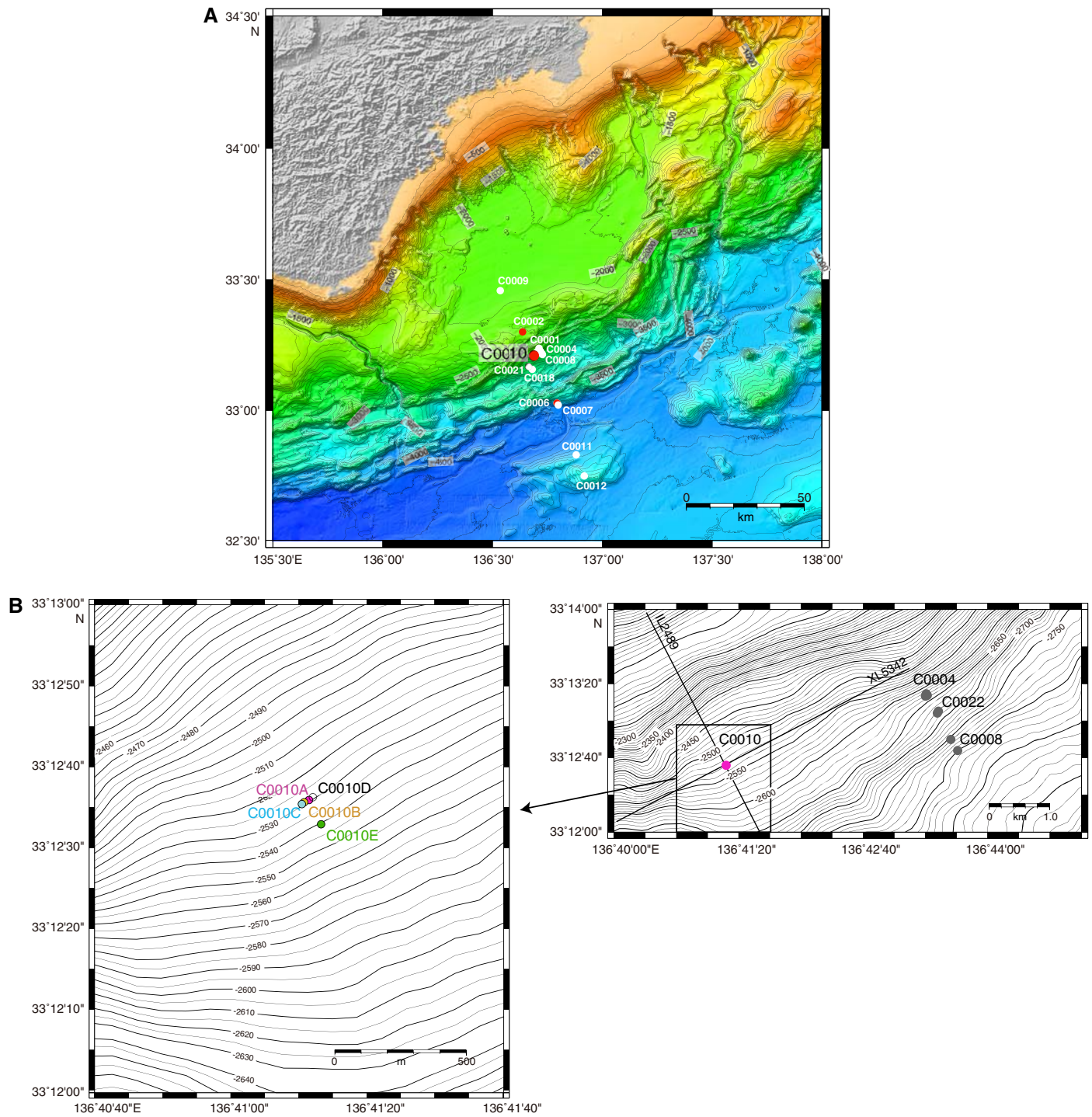
The Nankai Trough is formed by subduction of the Philippine Sea plate to the northwest beneath the Eurasian plate at a rate of ~40–60 mm/y (Figure F1; Seno et al., 1993; Miyazaki and Heki, 2001). The convergence direction is slightly oblique to the trench,

and sediments of the Shikoku Basin are actively accreting at the deformation front. The Nankai Trough is among the most extensively studied subduction zones in the world, and great earthquakes are well documented in historical and archaeological records (e.g., Ando, 1975). It has been a focus site for studies of seismogenesis by both the Integrated Ocean Drilling Program and the U.S. MARGINS initiative, based on the wealth of geological and geophysical data available.

The Nankai Trough has a 1300 y historical record of recurring great earthquakes that are typically tsunamigenic, including the 1944 Tonankai M8.2 and 1946 Nankaido M8.3 earthquakes (Ando, 1975; Hori et al., 2004). The rupture area and zone of tsunami generation for the 1944 event (within which the site of International Ocean Discovery Program [IODP] Expedition 365 is located) are now reasonably well understood (Ichinose et al., 2003; Baba et al., 2005, 2006). Land-based geodetic studies suggest that currently the plate boundary thrust is strongly locked (Miyazaki and Heki, 2001). Similarly, the relatively low level of microseismicity near the updip limits of the 1940s earthquakes (Obana et al., 2001) implies significant interseismic strain accumulation on the megathrust. However, recent observations of very low frequency (VLF) earthquakes within or just below the accretionary prism in the drilling area (Obara and Ito, 2005) demonstrate that interseismic strain is not confined to slow elastic strain accumulation. Slow slip phenomena, referred to as episodic tremor and slip, including episodic slow slip events and nonvolcanic tremor (Schwartz and Rokosky, 2007), are also widely known to occur in the downdip part of the rupture zone (Ito et al., 2007). In the subducting Philippine Sea plate mantle below the rupture zone, weak seismicity is observed (Obana et al., 2005). Seaward of the subduction zone, deformation of the incoming ocean crust is suggested by microearthquakes, as documented by ocean-bottom seismometer (OBS) studies (Obana et al., 2005).

The region offshore the Kii Peninsula on Honshu Island was selected for seismogenic zone drilling for several reasons. First, the rupture area of the most recent great earthquake, the 1944 Tonankai M8.2 event, is well constrained by recent seismic and tsunami waveform inversions (e.g., Tanioka and Satake, 2001; Kikuchi et al., 2003). Slip inversion studies suggest that only in this region did past coseismic rupture clearly extend shallow enough for drilling (Ichinose et al., 2003; Baba and Cummins, 2005), and an updip zone of large slip has been identified and targeted (Figure F2). Notably, coseismic slip during events such as the 1944 Tonankai earthquake may have occurred on the megasplay fault in addition to the plate boundary décollement (Ichinose et al., 2003; Baba et al., 2006). The megasplay fault is therefore a primary drilling target equal in importance to the basal décollement. Second, OBS campaigns and onshore high-resolution geodetic studies (though of short duration) indicate significant interseismic strain accumulation (e.g., Miyazaki and Heki, 2001; Obana et al., 2001). Third, the region offshore the Kii Peninsula is generally typical of the Nankai margin in terms of heat flow and sediment on the incoming plate. This is in contrast to the area offshore Cape Muroto (the location of previous scientific ocean drilling) where both local stratigraphic variations associated with basement topography and anomalously high heat flow have been documented (Moore et al., 2001, 2005; Moore and Saffer, 2001). Finally, the drilling targets are within the operational limits of riser drilling by the D/V *Chikyu* (i.e., maximum of 2500 m water depth and 7000 m subseafloor penetration). In the seaward portions of the Kumano Basin, the seismogenic zone lies ~4700–6000 m beneath the seafloor (Nakanishi et al., 2002).

Figure F1. A. Map showing locations of NanTroSEIZE drill sites (red = locations of existing and planned borehole observatory installations) (from Kopf, Araki, Toczko, and the Expedition 332 Scientists, 2011). Expedition 365 focuses on Site C0010, which penetrates the megasplay fault at 407 mbsf. B. Detail map showing location of Site C0010. IL = in-line, XL = cross-line.

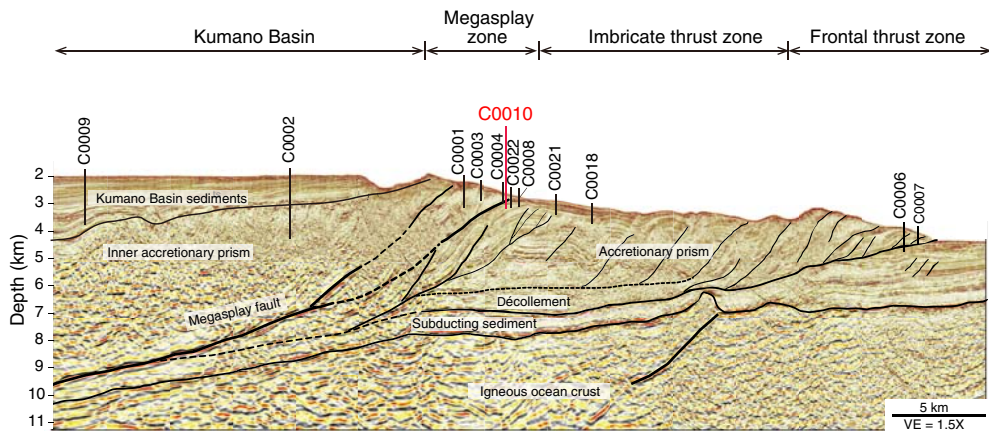


Seismic studies/site survey data

A significant volume of site survey data has been collected in the drilling area over many years, including multiple generations of 2-D seismic reflection (e.g., Park et al., 2002), wide-angle refraction (Nakanishi et al., 2002), passive seismicity, heat flow (Yamano et al., 2003), side-scan sonar, swath bathymetry, and submersible and remotely operated vehicle (ROV) dive studies (Ashi et al., 2002). In

2006, Japan and the United States conducted a joint 3-D seismic reflection survey over an ~11 km × 55 km area, acquired by PGS Geophysical, an industry service company (Moore et al., 2009). This 3-D data volume was the first deep-penetration, fully 3-D marine survey ever acquired for basic research purposes and has been used to (1) refine selection of drill sites and targets in the complex megasplay fault region, (2) define the 3-D regional structure and seismic

Figure F2. Interpreted seismic cross section of Kumano transect offshore and southeast of Kii Peninsula (modified from Moore et al., 2009; after Strasser et al., 2014). From the trench landward, the transect is separated into six morphotectonic domains: protothrust zone, frontal thrust zone, imbricate thrust zone, megasplay fault zone, Kumano Basin edge fault zone, and Kumano fore-arc basin. Drill sites on incoming Philippine Sea plate are not shown. VE = vertical exaggeration.



stratigraphy, (3) analyze physical properties of the subsurface through seismic attribute studies, and (4) assess drilling safety (Moore et al., 2007, 2009). These high-resolution 3-D data are being used in conjunction with physical property, petrophysical, and geo-physical data obtained from core analyses and both wireline and logging-while-drilling (LWD) logging to allow extensive and high-resolution integration of core, logs, and seismic data.

NanTroSEIZE drilling project

The NanTroSEIZE project is a multiexpedition, multistage IODP drilling project focused on understanding the mechanics of seismogenesis and rupture propagation along subduction plate boundary faults. The drilling program includes a coordinated effort to sample and instrument the plate boundary system at several locations offshore the Kii Peninsula (Tobin and Kinoshita, 2006a, 2006b; Figures F1, F2). The main objectives are to understand the following:

- The mechanisms and processes controlling the updip aseismic–seismic transition of the megathrust fault system,
- The processes of earthquake and tsunami generation,
- The mechanics of strain accumulation and release,
- The absolute mechanical strength of the plate boundary fault, and
- The potential role of a major upper plate fault system (termed the “megasplay” fault) in seismogenesis and tsunamigenesis.

The drilling program aims to evaluate a set of core hypotheses through riser and riserless drilling, long-term observatories, and associated geophysical, laboratory, and numerical modeling efforts. The following hypotheses are paraphrased from the original Integrated Ocean Drilling Program proposals and outlined in Tobin and Kinoshita (2006a, 2006b):

1. Systematic, progressive material and state changes control the onset of seismogenic behavior on subduction thrust faults.
2. Subduction megathrusts are weak faults.
3. Plate motion is accommodated primarily by coseismic frictional slip in a concentrated zone (i.e., the fault is locked during the interseismic period).

4. Physical properties of the plate boundary system (including the fault system and its hanging wall and footwall) change with time during the earthquake cycle.

5. A significant, laterally extensive upper plate fault system (the megasplay fault; Park et al., 2002) slips in discrete events that may include tsunamigenic slip during great earthquakes. It remains locked during the interseismic period and accumulates strain.

Sediment-dominated subduction zones such as the East Aleutian, Cascadia, Sumatra, and Nankai margins are characterized by repeated occurrences of great earthquakes of $\sim M8.0+$ (Ruff and Kanamori, 1983). Although the causal mechanisms are not well understood (e.g., Byrne et al., 1988; Moore and Saffer, 2001; Saffer and Marone, 2003) and great earthquakes are also known to occur within sediment-starved subduction zones such as the Japan Trench, the updip limit of the seismogenic zones at these margins is thought to correlate with a topographic break, often associated with the outer rise (e.g., Byrne et al., 1988; Wang and Hu, 2006). Along the Nankai margin, high-resolution seismic reflection profiles across the outer rise clearly document a large out-of-sequence thrust fault system (the megasplay fault, after Park et al., 2002) that branches from the plate boundary décollement close to the updip limit of inferred coseismic rupture in the 1944 Tonankai M8.2 earthquake (Figures F1, F2). Several lines of evidence indicate that the megasplay system is active and that it may accommodate an appreciable component of plate boundary motion. However, the partitioning of strain between the lower plate interface (the décollement zone) and the megasplay system, as well as the nature and mechanisms of fault slip as a function of depth and time on the megasplay are not understood. As stated in the fifth hypothesis above, one of the first-order goals in characterizing the seismogenic zone along the Nankai Trough, which bears both on understanding subduction zone megathrust behavior globally and on defining tsunami hazards, is to document the role of the megasplay fault in accommodating plate motion (both seismically and interseismically) and to characterize its mechanical and hydrologic behavior.

NanTroSEIZE Phase 1, conducted in 2007–2008, included three riserless drilling expeditions targeting the incoming sediments and ocean crust to characterize their physical properties, composition,

and state (pore pressure and temperature). Phase 2, conducted in 2009–2011, included (1) the first riser drilling in the Integrated Ocean Drilling Program at Site C0009 in the Kumano Basin, (2) observatory installations at Integrated Ocean Drilling Program Sites C0002 (long-term borehole monitoring system [LTBMS]) and C0010 (SmartPlug), and (3) additional riserless coring of subduction inputs and mass wasting deposits on the continental slope (Expedition 319 Scientists, 2010; Kopf, Araki, Toczko, and the Expedition 332 Scientists, 2011; Underwood et al., 2010; Henry, Kanamatsu, Moe, and the Expedition 333 Scientists, 2012). Phase 3, begun in 2010 and continuing with this expedition, includes riser drilling in Holes C0002F, C0002N, and C0002P (Tobin, Hirose, Saffer, Toczko, Maeda, Kubo, and the Expedition 348 Scientists, 2015) and installation of an LTBMS in Hole C0010A. To date, the NanTroSEIZE project has included 10 expeditions, encompassing a diverse suite of operations and lengths of individual expeditions, all conducted by the *Chikyu*.

NanTroSEIZE Stage 1 included three coordinated riserless drilling expeditions (Integrated Ocean Drilling Program Expeditions 314, 315, and 316). Eight sites were drilled across the continental slope and rise offshore the Kii Peninsula, many above the inferred coseismic slip region of the 1944 Tonankai M8.2 earthquake. The first Stage 1 expedition (314; LWD Transect) used LWD to define physical properties, lithostratigraphy, and structures in advance of coring operations (Kinoshita, Tobin, Ashi, Kimura, Lallemand, Screamton, Curewitz, Masago, Moe, and the Expedition 314/315/316 Scientists, 2009). This was followed by the first Center for Deep Earth Exploration (CDEX) coring expedition (315; Mega-Splay Riser Pilot) aimed at sampling the materials and characterizing in situ conditions within the hanging wall of the megasplay fault to a depth of 1000 meters below seafloor (mbsf) at Integrated Ocean Drilling Program Site C0001 and in the Kumano Basin fill and underlying accretionary wedge to a depth of 1057 mbsf at Site C0002 (Ashi et al., 2009). The third riserless expedition (316; Shallow Megasplay and Frontal Thrusts) targeted the megasplay at a depth of 350–400 mbsf (Integrated Ocean Drilling Program Site C0004) as well as the frontal thrust at the toe of the modern accretionary prism (Integrated Ocean Drilling Program Sites C0006 and C0007) (Screamton et al., 2009).

NanTroSEIZE Stage 2 operations began in 2009 with Integrated Ocean Drilling Program Expedition 319 (Riser/Riserless Observatory 1) followed by Integrated Ocean Drilling Program Expeditions 322 (Subduction Inputs), 332 (Riserless Observatory), and 333 (Subduction Inputs 2 and Heat Flow). Expedition 319 included (1) the first riser drilling in the Integrated Ocean Drilling Program (Site C0009), which penetrated the Kumano Basin fill and into accreted strata of the Nankai wedge overlying the locked subduction thrust, and (2) drilling across the shallow megasplay fault with LWD to a total depth (TD) of 555 mbsf at Site C0010 and installation of casing with screens positioned to span the megasplay at 407 mbsf (Expedition 319 Scientists, 2010). This hole was suspended with a temporary observatory attached to a retrievable bridge plug (termed the “SmartPlug”) to monitor temperature and pore pressure at the fault zone. Expedition 322 characterized the subduction inputs at Integrated Ocean Drilling Program Sites C0011 and C0012 (Underwood et al., 2010). Two more Stage 2 expeditions followed a year later. Expedition 332 recovered and replaced the temporary observatory at Site C0010 and deployed the first permanent LTBMS in Hole C0002G (Kopf, Araki, Toczko, and the Expedition 332 Scientists, 2011). Expedition 333 then conducted additional coring operations to complete the original objectives of Expedition 322 and to

sample mass wasting complexes on the continental slope (Henry, Kanamatsu, Moe, and the Expedition 333 Scientists, 2012).

NanTroSEIZE Stage 3 operations to date comprise three expeditions: Integrated Ocean Drilling Program Expeditions 326 (Plate Boundary Deep Riser 1), 338 (Plate Boundary Deep Riser 2), and 348 (Plate Boundary Deep Riser 3). Stage 3 has focused on riser drilling, with the ultimate objective of penetrating the megasplay fault at ~5000 mbsf. Expedition 326 drilled Hole C0002F to 827.5 mbsf to set shallow casing (Expedition 326 Scientists, 2011). Expedition 338 extended the hole to 2005 mbsf with LWD and also conducted riserless coring operations at Integrated Ocean Drilling Program Sites C0002, C0022, and C0021 (Strasser et al., 2014). Expedition 348 deepened Site C0002 in Holes C0002N and C0002P to a depth of 3056 mbsf (Tobin, Hirose, Saffer, Toczko, Maeda, Kubo, and the Expedition 348 Scientists, 2015) and included LWD as well as sampling cuttings and limited coring.

Expedition 365 is part of NanTroSEIZE Stage 3, with the primary objectives of (1) retrieving the temporary observatory at Site C0010 and (2) deploying a complex long-term observatory, which was connected to the Dense Oceanfloor Network System for Earthquakes and Tsunamis (DONET) seafloor cabled observatory network postcruise on 19 June 2016. Together with the existing observatory at Site C0002 and the anticipated future installation at Site C0006 (Figures F1, F2), the Site C0010 LTBMS allows monitoring within and above regions of contrasting behavior of the megasplay fault zone and plate boundary as a whole. These include a site above the updip edge of the “locked” zone (Site C0002), a shallow site in the megasplay fault zone and footwall (Site C0010; this expedition), and a site at the toe of the accretionary prism (Site C0006), where possible monitoring has been motivated by observed slip in the 11 March 2011 Tohoku earthquake that indicates coseismic rupture may propagate to the trench at some margins (e.g., Fujiwara et al., 2011). Together, the suite of NanTroSEIZE observatories has the potential to capture seismic and microseismic activity, slow slip, and interseismic strain accumulation along a transect from near-trench to the seismogenic zone. Such temporally continuous and spatially distributed observations are necessary to understand how each part of the plate boundary functions through the seismic cycle of megathrust earthquakes.

Scientific objectives and operational strategy

Background

Site C0010, located above the shallow megasplay fault and sited 3.5 km southwest of previously drilled Site C0004 (Figures F1, F2, F3), was originally drilled with LWD and cased during Expedition 319. Operations included drilling with measurement while drilling (MWD)/LWD across the megasplay fault to a TD of 555 mbsf, casing the borehole (with casing screens spanning the fault), conducting an observatory “dummy run” to test strainmeter and seismometer deployment procedures, and installing a simple temporary pore pressure and temperature monitoring system (SmartPlug) attached to a retrievable bridge plug (Expedition 319 Scientists, 2010). The hole was revisited during Expedition 332, when the SmartPlug was recovered and replaced with a similar temporary instrument package, which also included geochemical and microbiological sampling coils and an in situ microbiological colonization experiment; this temporary instrument package is termed the “GeniusPlug” (Kopf, Araki, Toczko, and the Expedition 332 Scientists, 2011; Figures F4, F5).

Figure F3. Detailed seismic reflection lines showing locations of Holes C0010A–C0010E. A. Dip line. B. Strike line. Line locations are shown in Figure F1B. mbsl = meters below sea level.

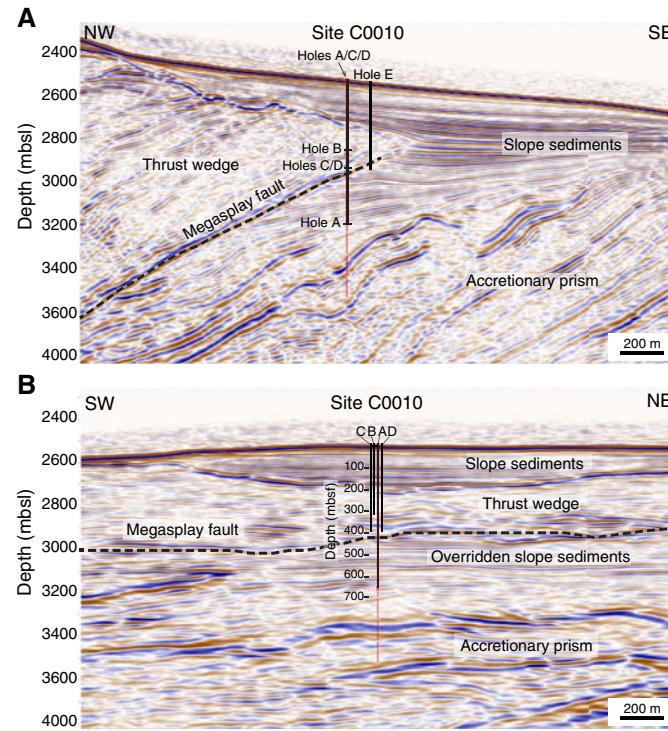
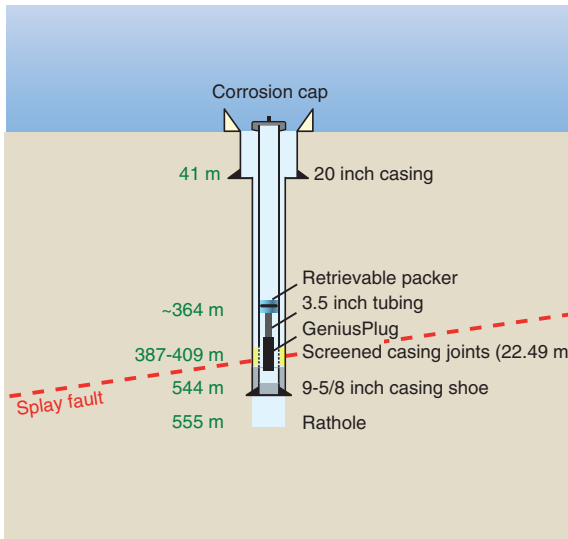
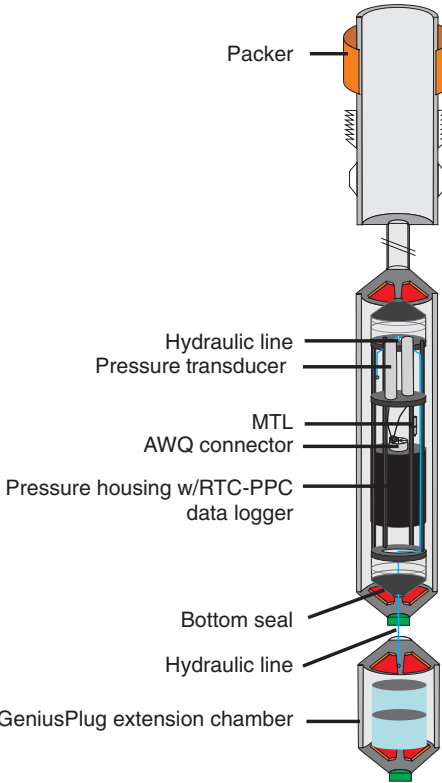


Figure F4. Schematic showing configuration of Hole C0010A and depths of GeniusPlug and key components of hole completion, Expedition 332.



Drilling during Expedition 319 identified three distinct lithologic packages at Site C0010, defined on the basis of LWD data, combined with coring and LWD at nearby Site C0004 (located 3.5 to the northeast along strike). From top to bottom, these lithologic packages are hemipelagic slope deposits composed primarily of mud with minor distal turbidite interbeds (Unit I, 0–182.5 m LWD depth below seafloor [LSF]), a thrust wedge composed of over-consolidated and fractured clay- and mudstones (Unit II, 182.5–407 m LSF), and overridden slope deposits (Unit III, 407 m LSF to TD).

Figure F5. GeniusPlug components. MTL = miniature temperature logger, AWQ = All Wet-mate QQ-C-465, RTC-PPC = real-time clock pressure period counter.



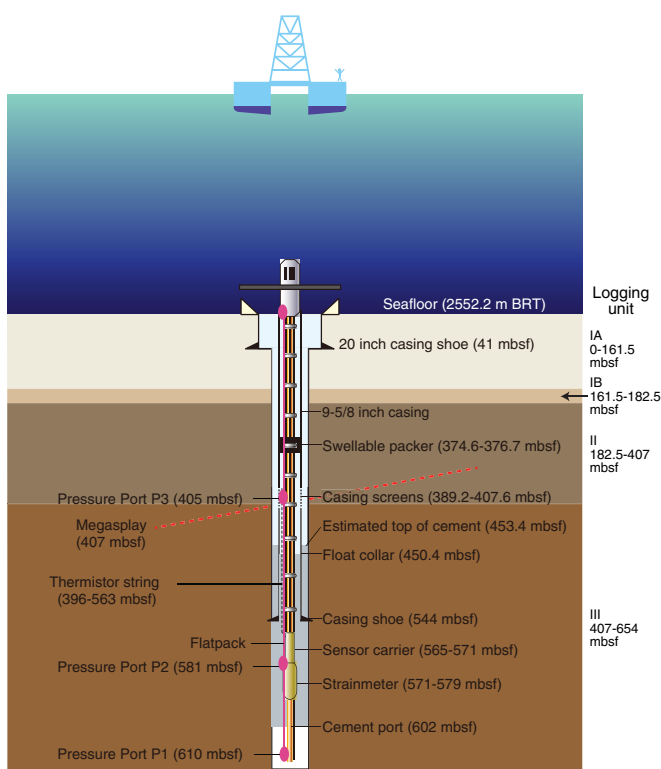
At Site C0010, logging Unit I is divided into two subunits: Subunit IA (0–161.5 m LSF), characterized by gamma ray and resistivity patterns similar to those observed in logging Unit I at Site C0004 (Expedition 314 Scientists, 2009), and Subunit IB (161.5–182.8 m LSF), interpreted as slope sediments composed of material reworked from the underlying thrust wedge.

For Expedition 365, the observatory system at Site C0010 consists of an array of sensors (Figure F6; see also **LTBMS** in the Expedition 365 methods chapter [Saffer et al., 2017a]) designed to monitor crustal deformation and hydrologic processes in the offshore portion of the subduction system over a wide range of time-scales. These monitoring targets include seismicity and microseismicity, slow slip events and VLF earthquakes, hydrologic transients, ambient pore pressure, and temperature. To allow the high sampling rates and ensure power delivery for the long-term and continuous monitoring necessary to capture this full range of events, the borehole observatory plans called for the observatory to be connected to the DONET submarine cable network (<http://www.jamstec.go.jp/donet/e>) after the drilling expedition in June 2016. The LTBMS installed at Site C0002 is also connected to this network, and the formation pressure data from either site can be viewed and downloaded at an open-access observatory data portal (<http://offshore.geosc.psu.edu>).

Scientific objectives

The primary plan for Expedition 365 was to recover the GeniusPlug installed in Hole C0010A during Expedition 332 (shown in Figure F5), deepen the hole from 555 to 655 mbsf, and install the LTBMS. Site C0010 constitutes the second LTBMS installation during NanTroSEIZE. The downhole configuration of the observa-

Figure F6. Schematic of LTBMS string installed in Hole C0010A after recovery of GeniusPlug. Logging units from Expedition 319 LWD runs in Hole C0010A are also shown for reference. BRT = below rotary table.



tory includes (1) pressure ports, (2) a volumetric strainmeter, (3) a broadband seismometer, (4) a tiltmeter, (5) three-component geophones, (6) three-component accelerometers, and (7) a thermometer array (Figure F6; see also **LTBMS** in the Expedition 365 methods chapter [Saffer et al., 2017a]). The observatory installation was planned to operate initially in a standalone mode at the well-head, using batteries and data recorders, with data recovery by subsequent ROV operations. On 19 June 2016, an ROV cruise downloaded initial data, conducted hydrostatic sensor checks for the pressure transducers, and connected the system to DONET so that measurements can be observed in real time from a shore-based monitoring station from that point onward.

Observatory operations went smoothly and much faster than planned, enabling us to conduct coring operations. This degree of contingency was not anticipated at the time of expedition planning, and as such, was not described in Kopf et al. (2015), and the expedition was not originally staffed for core sampling, measurements, or description. Description and analysis of the cores was therefore deferred to a shore-based sampling party on board the *Chikyu* in the port of Shimizu, Japan, in July–August 2016. The opportunity to collect cores introduced new science objectives for the expedition, including sampling of material from the hanging wall and footwall of the megasplay fault both for standard shipboard analyses and for subsequent shore-based study and characterization of the formation and interstitial fluids spanning the depth range of the screened casing. The latter of these objectives, in particular, has the potential to greatly enhance interpretations of the LTBMS and GeniusPlug data.

Specific objectives for Site C0010 during Expedition 365 were to

1. Recover the GeniusPlug installed in 2010 and conduct initial shipboard analyses of the recovered pore pressure and tempera-

ture data, fluids sampled by the sampling coils, and microbiological colonization experiment.

2. Deploy a LTBMS that includes pore pressure ports at three levels, a thermistor string, and a suite of geophysical instruments (strainmeter, tiltmeter, and seismometer) in a configuration like that in Hole C0002G (Kopf, Araki, Toczko, and the Expedition 332 Scientists, 2011). The detailed configuration of the LTBMS and borehole is described in **LTBMS** in the Expedition 365 methods chapter (Saffer et al., 2017a).
3. Drill, collect, and analyze core samples across the megasplay fault and spanning the interval of screened casing in Hole C0010A.

Operational strategy

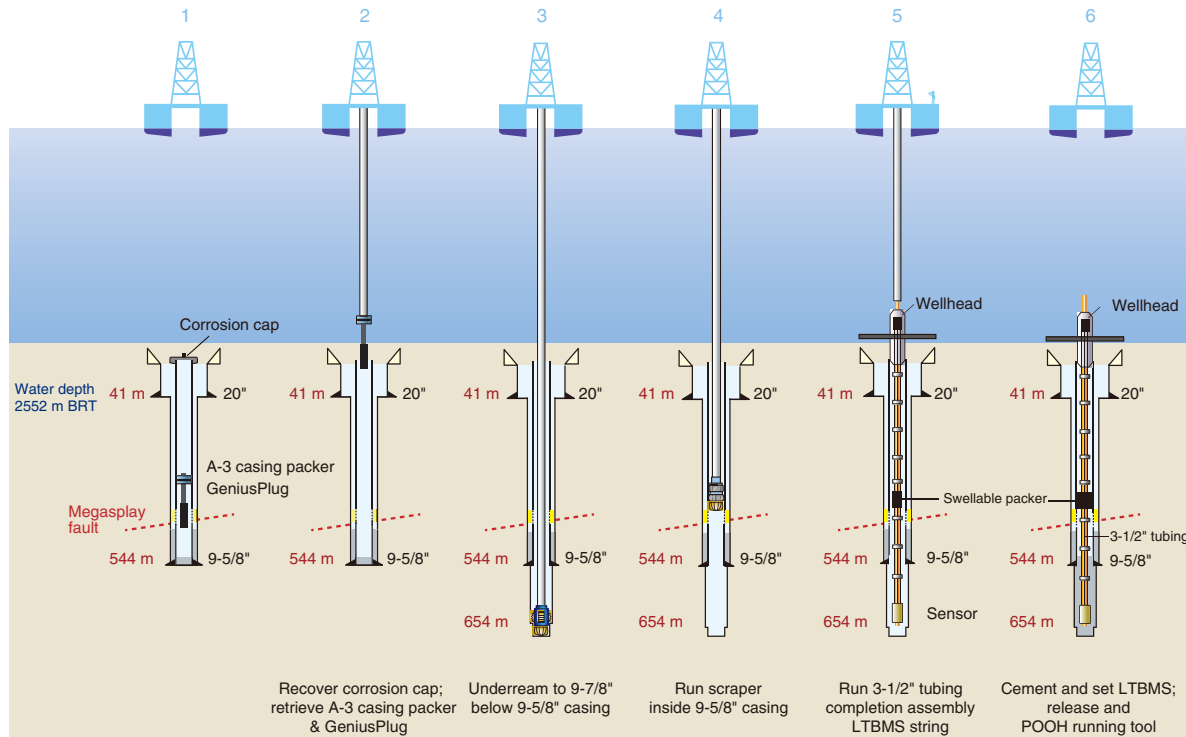
Planned work during Expedition 365 included two main operations at the cased borehole in Hole C0010A (Figure F7). The first operation was the recovery of the GeniusPlug. This was to begin following the transit from Shimizu Harbor to Site C0010 and after ROV dives to conduct a seafloor survey, set transponders, and remove the Hole C0010A well corrosion cap. Once complete, the vessel was to move away from the Kuroshio Current to a low-current area (LCA) to make up the GeniusPlug recovery bottom-hole assembly (BHA). The BHA consisted of the L-10 on/off tool, designed to recover the retrievable bridge plug from which the GeniusPlug was suspended. Once recovered from Hole C0010A, the vessel was to return to the LCA while the BHA was pulled out of the hole to the rig floor; the GeniusPlug would then be moved to the laboratory for data download, and the OsmoSampler/Flow-through Osmo Colonization System (FLOCS) experiment would be moved to the microbiology laboratory for sampling and analysis.

The next operation was to extend previously drilled Hole C0010A from 555 to 655 mbsf using a combination drill bit and underreamer BHA. Once drilling was finished, the drilling/underreaming BHA was to be pulled out of the hole and replaced with a scraper BHA to ensure the cased section of the well was clear of any obstructions. The expedition science objectives would be completed with operations to deploy the LTBMS. This involved considerable moonpool preparation using newly developed guide rollers to run the completion.

A major impediment to observatory deployment in the Nankai region is the extremely strong Kuroshio Current. Current speeds up to 6 kt are possible, and the current flow past the drill string commonly results in vortex-induced vibration (VIV), which has caused lost drill pipe, dropped casing, and destroyed electronic sensors during past Integrated Ocean Drilling Program expeditions (Expedition 319 Scientists, 2010). CDEX has developed a series of mitigation techniques and equipment to minimize or suppress VIV. These include the attachment of ropes to drill string sections exposed to the current, preventing the formation of vortices as the current flows past the drill string. Other newly developed tools are the moonpool guide rollers, which support the drill string in the moonpool and provide a safe platform for moonpool work, and guides for attaching the VIV-suppressing ropes, cables, and hydraulic flatpack lines to the LTBMS observatory instruments.

The operational plan called for the LTBMS to be made up from the bottom bullnose to the seafloor LTBMS head as the completion was run into the moonpool. A series of system checks on the status of the strainmeter, tiltmeter, broadband seismometer, and pressure sensor unit (PSU) were to be performed at set stages as the LTBMS and sensors were assembled. Once the LTBMS was completed and run into the water, the *Chikyu* would then drift back into the Kuro-

Figure F7. Operations sequence, Hole C0010A. POOH = pull out of hole.



shio Current to run the LTBMS into Hole C0010A. After checking that all systems were working, the LTBMS would be cemented in place, and the vessel would release the LTBMS running tool and recover the drill string.

Coring operations were planned to maximize limited available time in order to target the key interval spanning the megasplay fault and the screened casing zone and to penetrate and sample the footwall. For this reason, in Hole C0010B (abandoned due to bad hole conditions after a single core with no recovery) and subsequently in Hole C0010C we planned to drill without coring to 300 mbsf and to then core across the fault (located at 407 mbsf in Hole C0010A as identified by LWD data). In Hole C0010C, coring reached 395 mbsf before hole conditions deteriorated, requiring that we abandon the hole. For Holes C0010D and C0010E, the coring strategy was modified in light of limited remaining operational time. For these holes, we planned to drill without coring to a depth closer to the anticipated fault and then begin coring from ~15 to 20 m above the megasplay and into the footwall. This depth was 385 mbsf in Hole C0010D and 360 mbsf in Hole C0010E, where the megasplay was shallower because the hole was located ~100 m up-dip of Holes C0010A–C0010D (cf. Figure F3).

Operations

Port call and transit to Site C0010

Expedition 365 began in the port of Shimizu, Shizuoka Prefecture, Japan, on 26 March 2016. The first few days were spent quay-side, loading cargo and supplies. The science party boarded the *Chikyu* on 27 March and participated in the shipboard prespud meeting on 28 March. The *Chikyu* sailed from Shimizu Harbor at 0900 h on 29 March (see Table T1 in the Site C0010 chapter [Saffer et al., 2017b]), lowered the azimuth thrusters, and arrived on location at Site C0010 at 0330 h on 30 March.

Site C0010

While the supply boat searched for the Kuroshio Current edge, the ROV dove to survey the seabed, set transponders, and remove the corrosion cap. The *Chikyu* moved to the LCA to begin running the BHA in the hole (see Table T2 in the Site C0010 chapter [Saffer et al., 2017b]) from 2145 h. The science party placed an accelerometer on the drill string to evaluate the Kuroshio Current VIV as preparation for GeniusPlug recovery and LTBMS operations.

The *Chikyu* reached the LCA 12 nmi northwest of Site C0010 at 0000 h on 31 March 2016 and began drifting back to the well center. At 1136 h on 1 April, an M6.0 earthquake struck, with the reported hypocenter ~10 nmi to the northwest of Site C0010 and 15 km deep. The earthquake was felt aboard the ship. Running drill pipe resumed, and on 1 April, the L-10 BHA was over the wellhead and was stabbed in. The BHA landed on the bridge plug and the drill string rotated to release the mechanical seal. The bridge plug and the GeniusPlug successfully cleared the wellhead at 2040 h. The L-10 BHA was pulled out of the hole as the *Chikyu* moved toward the LCA to recover the BHA and GeniusPlug on deck. The L-10 tool, the bridge plug, and the GeniusPlug were recovered on deck at 0500 h on 3 April. The OsmoSampler portion of the GeniusPlug was opened, and the FLOCS and OsmoSampler experiments were moved to the microbiology laboratory.

The *Chikyu* began drifting to the LCA 8 nmi west of Site C0010 and began rigging up the guide horn in preparation for drilling out the cement plug. From early on 4 April (0100 h), the drilling and underreaming BHA was assembled and run in the hole (see Table T2 in the Site C0010 chapter [Saffer et al., 2017b]). Drilling out the cement started from 1200 h on 4 April. Once drilling out cement was completed, the underreamer was activated and opened the hole until reaching TD (654 mbsf; 3206 m below rotary table [BRT]) at 1945 h. A short wiper trip confirmed no excessive overpull or

torque. The underreamer BHA was pulled out of the hole, reaching the deck by 5 April. The 9% inch casing scraper BHA was made up and run in the hole (see Table T2 in the Site C0010 chapter [Saffer et al., 2017b]). The BHA was stabbed into the Hole C0010A wellhead and scraped to 2934 m BRT. The scraper BHA was pulled out of the hole and laid down by 0900 h on 6 April. The guide horn was rigged down, and preparations for running the LTBMS completion began. However, the approach of a cold front necessitated waiting on weather until 0245 h on 8 April. At that time, LTBMS preparations were restarted.

The LTBMS completion string was run in the hole, and miniscreens for pressure Port P1, cables, and sensors were attached to the completion string. On the morning of 9 April, the sensor cables were connected to the strainmeter, seismometer, and thermistor. Testing revealed that the strainmeter and seismometer were faulty, so the LTBMS was pulled out of the hole to the rig floor to replace the faulty sensors with standby instruments. The testing cable was also identified to be faulty and was therefore replaced. Assembly of the replacement sensors and LTBMS was completed by 1615 h, and the LTBMS completion was run in the hole, pausing on 10 April to install the swellable packer in the moonpool from 1815 h. The LTBMS head and hydraulically activated running tool (HART) (see Table T2 in the Site C0010 chapter [Saffer et al., 2017b]) were picked up then made up to the rest of the LTBMS completion assembly and lowered into the moonpool by 1700 h on 11 April. There, the stainless steel hydraulic $\frac{1}{4}$ inch lines leading from the PSU mounted on the LTBMS head were connected to the flatpack running down to the pressure ports. The PSU valves were kept “open” to prevent damage during running. The sensor cables were measured and prepared for termination at Teledyne Oil and Gas ODI connectors by 12 April. A data logger and battery unit was mounted on the ROV platform to collect data until the planned connection to DONET.

The LTBMS completion assembly was run into the water, and by 1000 h on 14 April the vessel was back at Site C0010. The LTBMS completion assembly reentered the Hole C0010A wellhead. The ROV moved the PSU 2-way valves from open to “closed” to protect the lines from fouling during landing, circulation, and cementing. The LTBMS head was landed by 0515 h on 15 April. Cementing was finished by 1045 h. The HART was released from the LTBMS and pulled out of the hole, and on 15 April the BHA was laid down on the rig floor by 2300 h. The moonpool completion guide, completion guide roller, and VIV-suppression rope drums were removed from the working cart and blowout preventer cart so that rigging up the guide horn could begin for coring operations at Site C0010. A series of 10 sensor health checks (see Table T1 in the Site C0010 chapter [Saffer et al., 2017b]) were run on the sensors at specific stages during the assembly and running of the LTBMS. Except for the sensor failure noted above, all health checks were positive.

Contingency coring operations were originally planned to test the Turbine Driven Coring System developed by CDEX in preparation for deep coring operations. However, after considering the large amount of expedition time remaining, the Co-Chief Scientists, Expedition Project Manager, and Operations Superintendent all agreed to move forward with rotary core barrel (RCB) coring in order to maximize potential science return. Coring was conducted in four holes, all of which were drilled down without coring to ≥ 300 mbsf: Holes C0010B (300–309.5 mbsf), C0010C (300–395 mbsf), C0010D (385–394.5 mbsf), and C0010E (360–391 mbsf). Coring was most successful in Hole C0010C (Table T1) with 52.6 m of core collected for a 95 m advance (55.4% recovery). Core recovery rates tended to increase with depth in both Holes C0010C and C0010E. There were problems with borehole stability, and these required abandoning each hole with the exception of Hole C0010E. Core recovery continued to be high at this site, but because the drawworks needed scheduled maintenance, the consensus was to halt coring

Table T1. Site C0010 coring details. MSL = from mean sea level. [Download table in .csv format.](#)

Hole	Longitude	Latitude	Seafloor depth BRT (m)	Water depth MSL (m)	Core	Core on deck date (2016)	Core on deck time (h)	Top depth BRT (m)	Bottom depth BRT (m)	Top depth (mbsf)	Bottom depth (mbsf)	Advanced interval (m)	Recovered interval (m)	Recovery (%)	Time on hole (h)
C0010B	33°12.5930'N	136°41.1806'E	2554.0	2525.5	1R	17 Apr	0930	2854.0	2863.5	300.0	309.5	9.5	0	0	
						Hole C0010B totals:		2854.0	2863.5	300.0	309.5	9.5	0	0	3.25
C0010C	33°12.5899'N	136°41.1748'E	2553.0	2524.5	1R	18 Apr	0417	2853.0	2862.5	300.0	309.5	9.5	5.49	57.8	
					2R	19 Apr	0655	2862.5	2872.0	309.5	319.0	9.5	5.18	54.5	
					3R	19 Apr	0925	2872.0	2881.5	319.0	328.5	9.5	3.85	40.5	
					4R	19 Apr	1216	2881.5	2891.0	328.5	338.0	9.5	3.34	35.2	
					5R	19 Apr	1533	2891.0	2900.5	338.0	347.5	9.5	3.81	40.1	
					6R	19 Apr	1855	2900.5	2910.0	347.5	357.0	9.5	5.18	54.5	
					7R	20 Apr	0045	2910.0	2919.5	357.0	366.5	9.5	6.78	71.4	
					8R	20 Apr	0419	2919.5	2929.0	366.5	376.0	9.5	3.41	35.9	
					9R	20 Apr	0706	2929.0	2933.5	376.0	380.5	4.5	3.88	86.2	
					10R	20 Apr	1027	2933.5	2938.0	380.5	385.0	4.5	5.22	116.0	
					11R	20 Apr	1404	2938.0	2943.0	385.0	390.0	5.0	4.07	81.4	
					12R	20 Apr	1912	2943.0	2948.0	390.0	395.0	5.0	2.38	47.6	
					Hole C0010C totals:		2943.0	2948.0	390.0	395.0	95.0	52.6	55.4		46.50
C0010D	33°12.6024'N	136°41.2042'E	2555.0	2526.5	1R	22 Apr	2054	2940.0	2949.5	385.0	394.5	9.5	7.22	76.0	
					Hole C0010D totals:		2940.0	2949.5	385.0	394.5	9.5	7.22	76.0		0.25
C0010E	33°12.5500'N	136°41.2223'E	2566.5	2538.0	1R	23 Apr	2316	2926.5	2932.5	360.0	366.0	6.0	0.22	3.7	
					2R	24 Apr	0048	2932.5	2938.5	366.0	372.0	6.0	3.03	50.5	
					3R	24 Apr	0230	2938.5	2948.0	372.0	381.5	9.5	10.1	106.3	
					4R	24 Apr	0407	2948.0	2957.5	381.5	391.0	9.5	8.73	91.9	
					Hole C0010E totals:		2948.0	2957.5	381.5	391.0	31.0	22.1	71.2		7.25
					Site C0010 coring totals:		2943.0	2949.5	390.0	395.0	145.0	81.9	56.5		57.25

Table T2. Summary of drilling, LTBMS installation, and coring during Expedition 365. NA = not applicable. [Download table in .csv format.](#)

Hole	Latitude	Longitude	Water depth BRT (m)	Water depth MSL (m)	Operation	Drilled interval (mbsf)	Cased interval (mbsf)	Total penetration (m)	Cores (N)	Core interval cored (m)	Core recovered (m)	Recovery (%)	Time on hole (days)
C0010A	33°12.5981'N	136°41.1924'E	2552	2523.5	GeniusPlug recovery Hole extension, LTBMS deployment	0.0 129.0	544.3 NA	0.0 654.0	NA NA	NA NA	NA NA	NA NA	3 13.7
C0010B	33°12.5930'N	136°41.1806'E	2554	2525.5	Coring (RCB)	309.5	NA	309.5	1	9.5	0.0	0.0	2.3
C0010C	33°12.5899'N	136°41.1748'E	2553	2524.5	Coring (RCB)	300.0	NA	395.0	12	95.0	52.6	55.4	2.7
C0010D	33°12.6024'N	136°41.2042'E	2555	2526.5	Coring (RCB)	380.0	NA	394.5	1	9.5	7.2	76.0	2
C0010E	33°12.5500'N	136°41.2223'E	2566.5	2538.0	Coring (RCB)	360.0	NA	391.0	4	31.0	22.1	71.2	1.5
					Expedition 365 totals:	1118.5	544.3	1753.0	18	145.0	81.9	56.5	25

operations once major targets were reached. With the recovery of the RCB BHA on deck, science operations for Expedition 365 were completed (Table T2). The *Chikyu* returned to Shimizu Harbor on 27 April and lowered the gangplank at 1030 h.

Because of the core recovered, a shore-based sampling party was held aboard the *Chikyu* while quayside in Shimizu, Japan, from 25 July to 5 August 2016.

Principal results

GeniusPlug

One of the primary objectives of Expedition 365 was to recover the GeniusPlug temporary observatory from Hole C0010A (Figures F8, F9; see also Figure F4) and conduct initial analyses of the pressure and temperature data, fluid geochemical samples collected in both chemical and biological sampling coils, and FLOCS for microbiology. All of these data and samples were successfully recovered from the instrument package, although a significant fraction of fluids in the chemical and biological sampling coils was lost upon depressurization during ascent through the water column and on the rig floor.

The pressure and temperature records clearly document several key events during the ~5.3 y deployment period (November 2010 through April 2016). Initial analysis of the data illustrates two principal results. First, on the basis of hydraulic isolation of the formation (downward looking) and hydrostatic reference (upward looking) sensors, it is clear that the bridge plug successfully sealed, and thus that the downward-looking sensor provides a meaningful record of formation pressure. This is most evident at the start and end of the deployment when the bridge plug was set and retrieved, respectively. In both cases, the hydrostatic pressure record exhibits large perturbations associated with drill string movement and attaching/detaching the running tool, whereas the downward-looking pressure record is stable (Figure F10). Additionally, initial review of the pressure-time series documents clear responses to several regional and local earthquakes. These include the 11 March 2011 Tohoku M9 and 1 April 2016 Mie-ken Nanto-oki M6 earthquakes (Figures F11, F12). The latter event occurred below and slightly landward of Site C0010 and is manifested as the arrival of a wave-train followed by a distinct pressure increase of ~0.4 kPa, likely indicating compressional coseismic strain. For both events, the subsequent tsunami wave is also clearly recorded in both the seafloor and formation sensors. These examples serve to highlight the ability of offshore borehole observatory systems to sense a wide

Figure F8. Photo of GeniusPlug after recovery. P = pressure.



Figure F9. OsmoSampler coils.

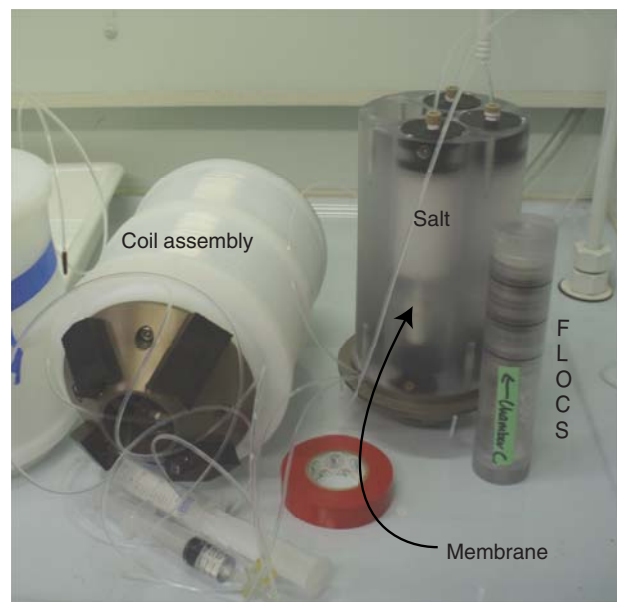


Figure F10. Pressure records from GeniusPlug deployment. A. Overview of entire deployment period. B. Installation time window. C. Instrument recovery period.

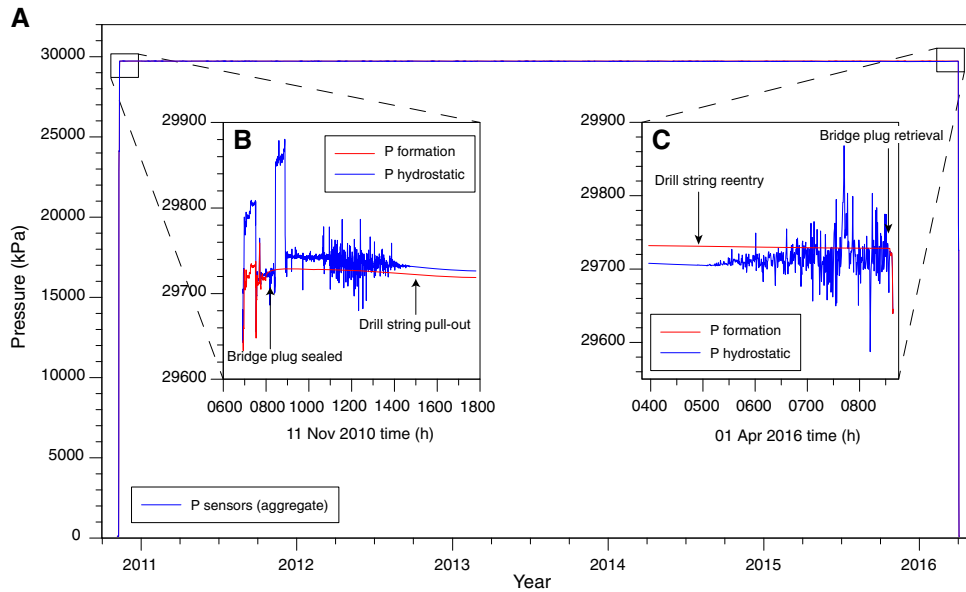
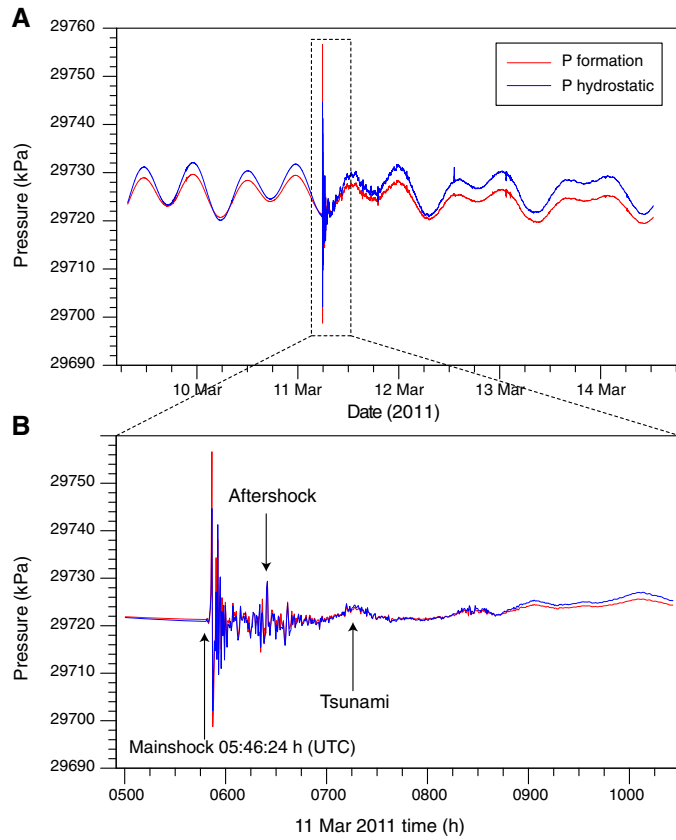


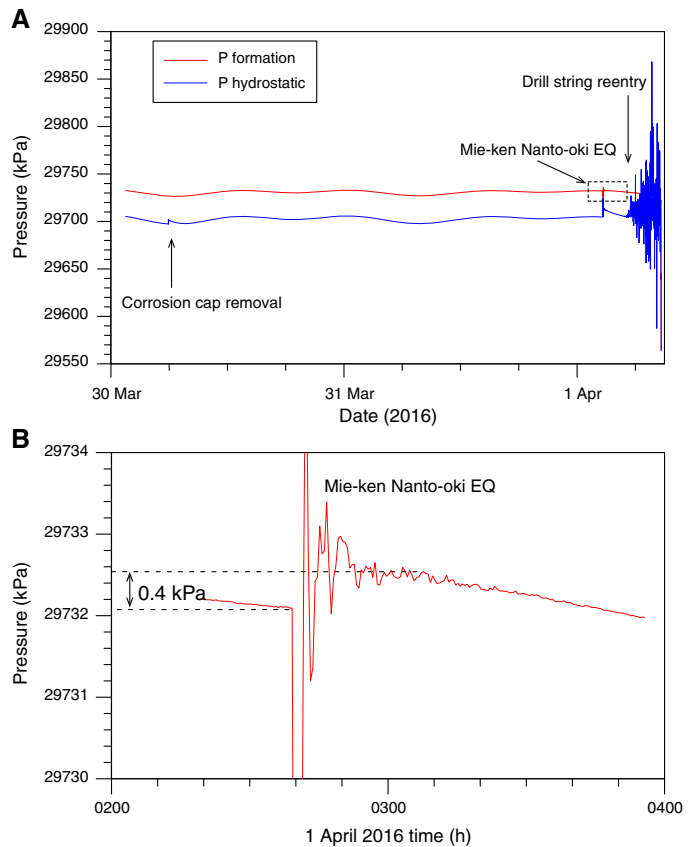
Figure F11. Pressure records for the 11 March 2011 Tohoku M9 earthquake. A. Data from 9 to 15 March 2011. B. Earthquake record on 11 March 2011.



range of crustal strain processes and to enable detailed characterization by monitoring in the near-field.

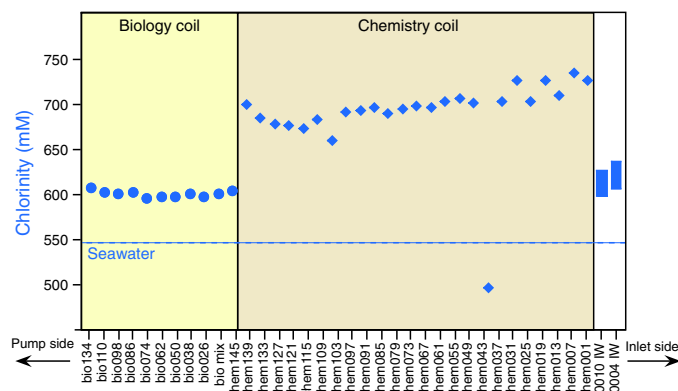
Analysis of the GeniusPlug fluid samples indicates that, for many elements (e.g., Cl, K, Ca, and Br), the fluids sampled by the OsmoSampler coils are broadly consistent with formation pore flu-

Figure F12. Pressure records for the 1 April 2016 Mie-ken Nanto-oki M6 earthquake (EQ). A. 2.3 day period from 30 March to 1 April 2016. B. Time window of earthquake.



ids measured from cores at both Sites C0004 and C0010 (Figure F13). However, some key differences were also observed between the two sets of samples and between the GeniusPlug fluid samples and previously collected interstitial pore waters. The biology coils,

Figure F13. Chlorinity data from GeniusPlug chemistry (chem) and biology (bio) coils. Interstitial water (IW) results for Sites C0004 and C0010 are shown for comparison.



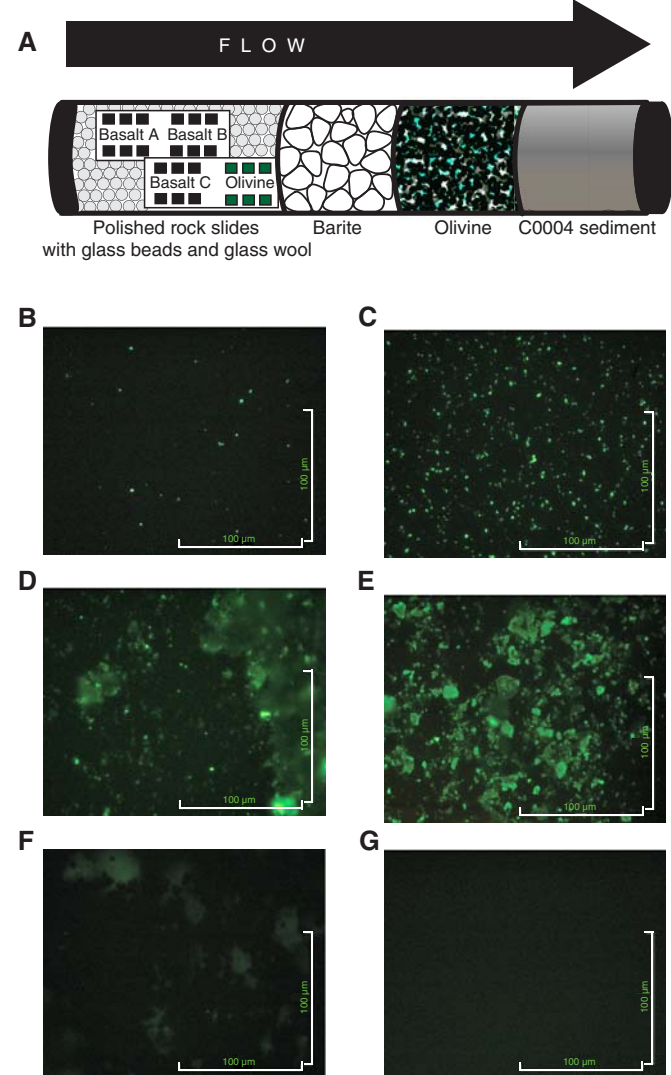
which drew fluid from the screened interval of the borehole then through the FLOCS unit and into the sampling coil, exhibit elevated B and SO_4 and reduced Ba concentrations relative to the chemical coils, which drew water directly from the borehole. Reduced Ba are consistent with barite precipitation in the FLOCS unit, whereas the lower SO_4 in the chemistry coil may reflect microbial uptake of sulfate in the chemical coil due to unanticipated colonization of the membrane itself. Gradually increasing salinity in the chemical coil toward the inlet may reflect an artifact caused by leakage across the membrane in the chemistry unit's pump.

The OsmoSampler and FLOCS (Figure F14A) provided an opportunity to sample native microbial communities living in the pervasively fractured thrust wedge, with the advantage that pristine in situ fluids and microbes could be collected without drilling-induced contamination. This marked the first deployment of a FLOCS unit in a sedimentary environment. When the OsmoSampler and FLOCS unit were recovered, substrates were subsampled for DNA analyses, microscopy, and culture experiments. The culture experiments were initiated on board and inoculated with substrates of the FLOCS. The observed growth from these cultures—and not the controls—suggests that the FLOCS successfully collected viable microorganisms (Figure F14B–F14G), validating the use of OsmoSampler and FLOCS technology in sedimentary environments. Future shore-based DNA analyses will further characterize these microbial communities and their metabolic potentials.

LTBMS installation

As described in **Scientific objectives**, from bottom to top the LTBMS included (see Figure F6) hydraulic ports to monitor pore fluid pressure in an open hole interval spanning from 602 mbsf to the TD of 654 mbsf; a volumetric strainmeter (572–580.6 mbsf); a tilt combo package that includes a broadband seismometer, geophone, accelerometer, tiltmeter, and a thermistor string mounted on a sensor carrier (565–572 mbsf); and an upper hydraulic port to monitor pore pressure in a screened interval spanning the megasplay fault (Figures F15, F16, F17). The thermistor string data logger was mounted on the sensor carrier; however, the string itself consisted of 5 thermistors spanning from 396 to 563 mbsf. In addition, a hydraulic port was included in the instrument carrier-strainmeter assembly, which was to be cemented in the hole (Figure F6). The three hydraulic lines were encased in urethane within a single umbilical flatpack and broken out for termination at each of the three downhole port locations. A swellable packer set above the

Figure F14. A. Schematic of FLOCS unit. B–G. Microscope images, with micro-organisms stained green. Inoculum for each culture: (B) FLOCS fluids, (C) crushed barite, (D) Site C0004 sediment, (E) olivine, (F) rust from Genius-Plug casing, and (G) control.



screened casing interval provides hydraulic isolation between the upper pressure port and the overlying ocean. Taken together, the suite of instruments enables measurement of crustal deformation over a wide bandwidth (from 0.01 s to several months or longer) with the high precision needed to detect earthquakes, microseismicity, low frequency earthquakes, and slow slip events.

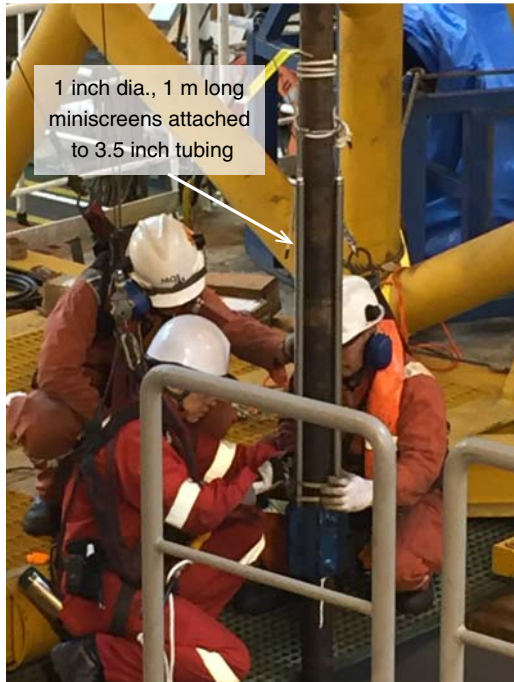
The locations of the sensors in the array were chosen on the basis of logging data from Expedition 319 and further guided by comparison with coring results from Site C0004 located 3.5 km to the east-northeast along strike (Screaton et al., 2009; Expedition 319 Scientists, 2010) (Figure F6). The lowermost pressure port is located within overridden slope sediments in the footwall of the megasplay fault (logging Unit III). The strainmeter and instrument carrier are also installed within logging Unit III. The total thermistor string length is 175 m, with the two uppermost nodes located within the screened casing interval, two more below the screened interval, and the bottom node just above the instrument carrier.

The completion string for the LTBMS was prepared by attaching the sensors, cables, pressure ports, and hydraulic lines to 3½ inch

Figure F15. LTBMS head, showing configuration of each bay (top) and ROV platform and data recorder (bottom).

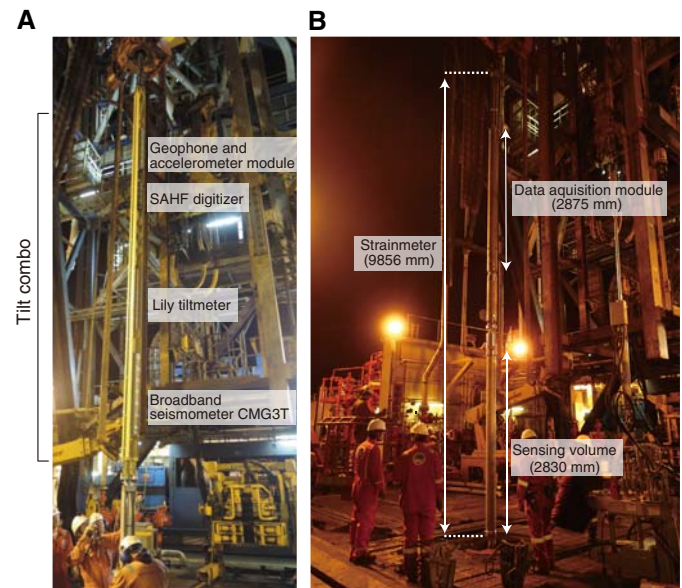


Figure F16. Miniscreens used to terminate hydraulic line at the lowermost pressure port.



tubing. The top of the string was terminated at the LTBMS head where underwater mateable connectors (UMC) and hydraulic lines

Figure F17. A. Instrument carrier. SAHF = stand-alone heat flow. B. Strainmeter suspended in moonpool.



with valves and the PSU were mounted (Figure F15). An ROV platform was attached to the wellhead prior to lowering the wellhead into water. A titanium sphere data recorder and communications unit with three UMC hoses connected to each downhole sensor was also installed on the ROV platform. At the time of initial assembly, the PSU began continuous recording to its stand-alone data logger with a 1 min sampling interval. The hydraulic valves on the LTBMS head were set to connect the pressure gauges in the PSU to the overlying ocean but isolated from the formation hydraulic lines to avoid potential damage to the sensors due to pressure fluctuations during landing and cementing operations. The other sensors were not recording at this time.

Assembly was conducted in a LCA to avoid potential vibration and damage caused by lowering the string through the Kuroshio Current. VIV was also suppressed by attaching ropes to the drill string while deploying and drifting (Kopf, Araki, Toczko, and the Expedition 332 Scientists, 2011). Additionally, newly developed moonpool equipment, including guide rollers and completion guide rollers, were used to more efficiently and smoothly attach the hydraulic umbilical and cables (guide roller) and ropes (completion guide roller). Throughout the deployment sequence (i.e., string assembly, lowering, drifting, reentry, landing, and cementing), a series of communication tests were conducted with the borehole instruments to verify sensor and cable function.

After landing the LTBMS, we initialized the data recorder to start data acquisition for the tilt combo package and strainmeter. The ROV maintained a connection to the data recorder at this time to monitor the status of the sensors during cementing. Temperature records during this period document cooling of the borehole due to circulation. Pressure recorded at the strainmeter port indicates a pressure increase of ~0.7 MPa during cementing, indicating that 78 m of seawater above the pressure sensor was displaced by the denser cement. After cementing was complete, the hydraulic valves at the LTBMS head were turned to connect the pressure gauges to the formation hydraulic lines, and initial pressure data spanning the descent through the water column and LTBMS head landing were downloaded by the ROV. The PSU logger memory was then cleared,

and valve configurations and positions of all instruments installed on the ROV platform were checked by visual inspection prior to leaving the site.

Coring

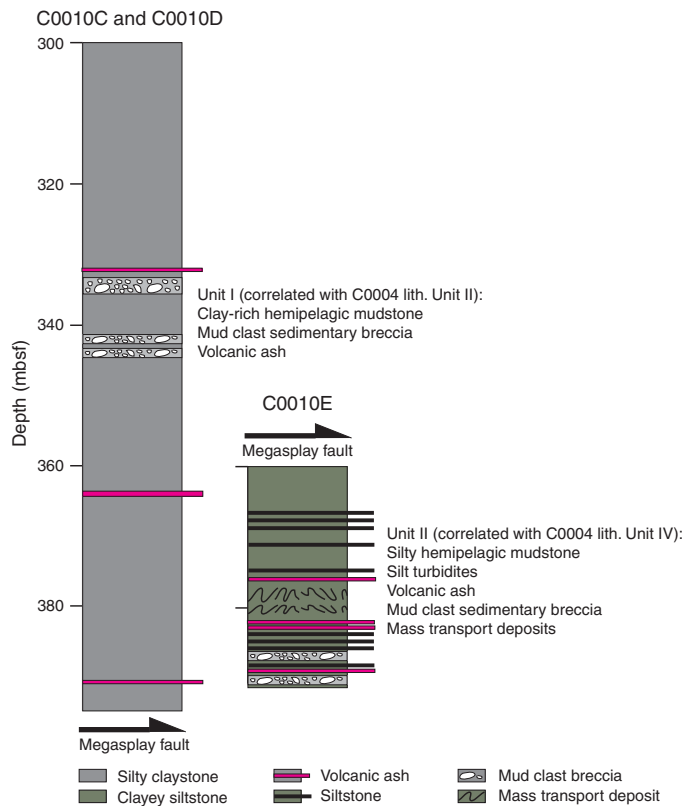
Coring operations were conducted in four holes: C0010B–C0010D, located within 30 m and offset along strike from Hole C0010A, and Hole C0010E, offset 95 m to the south-southeast in the updip direction where the thrust wedge is thinner and the megasplay fault is shallower (Figures F1A, F3). Because coring operations were not anticipated and were not part of the primary expedition plan, the shipboard laboratory technicians and science party were not staffed to split, describe, or sample cores. For this reason, whole (unsplit) cores were sampled for headspace gas analyses and immediately scanned with X-ray computed tomography to identify candidate intervals for time-sensitive whole-round sampling. After taking whole-round samples for interstitial water and microbiology, the cores were run through the whole-round multi-sensor core logger and then refrigerated. All further shipboard analyses and sampling were deferred until a sampling party conducted on the *Chikyu* while in port in Shimizu, Japan, from 25 July to 5 August 2016.

Coring in Holes C0010C and C0010D recovered fractured silty claystone from depths corresponding to the hanging wall of the megasplay (<400 mbsf) and in the age range 3.79–5.59 Ma. Core samples collected from Hole C0010E span the interval from 360 to 391 mbsf and primarily recovered clayey siltstones from the footwall of the fault, with ages from 1.56 to 1.67 Ma (Figure F18). The hanging wall to the megasplay fault (Holes C0010C and C0010D) is dominated by indurated, gray to greenish gray silty claystone. The silty claystone is mottled by bioturbation where intact but more typically overprinted by deformation and coring disturbance, with many intervals of dense fractures and drill breccia. Subordinate lithologies include thin beds of gray vitric ash. The ash is locally entrained along fractures and faults. This unit also contains intervals of sedimentary breccia with subrounded to subangular clasts of remobilized mudstone supported by a mudstone matrix. X-ray diffraction (XRD) data show high percentages of total clay minerals relative to quartz and feldspar.

The footwall to the megasplay fault contains olive-gray clayey siltstone that is weakly indurated and consistently coarser grained than strata in the hanging wall. Bioturbation and faint laminae are widespread. Thin interbeds of dark gray silt are common, typically with sharp bases, normal size grading, and plane-parallel laminae. Thin interbeds of light to medium gray vitric ash are also common. Some intervals in the footwall display contorted soft-sediment deformation, with highly variable dips to laminae, clasts of remobilized mudstone, and pebble- to granule-sized lithic fragments and pumice supported by a matrix of silty claystone. XRD data show consistent increases in the relative percentages of quartz and feldspar relative to the hanging wall.

Bedding in Holes C0010C and C0010D, in the hanging wall of the megasplay fault, is near horizontal or gently dipping from 300 to

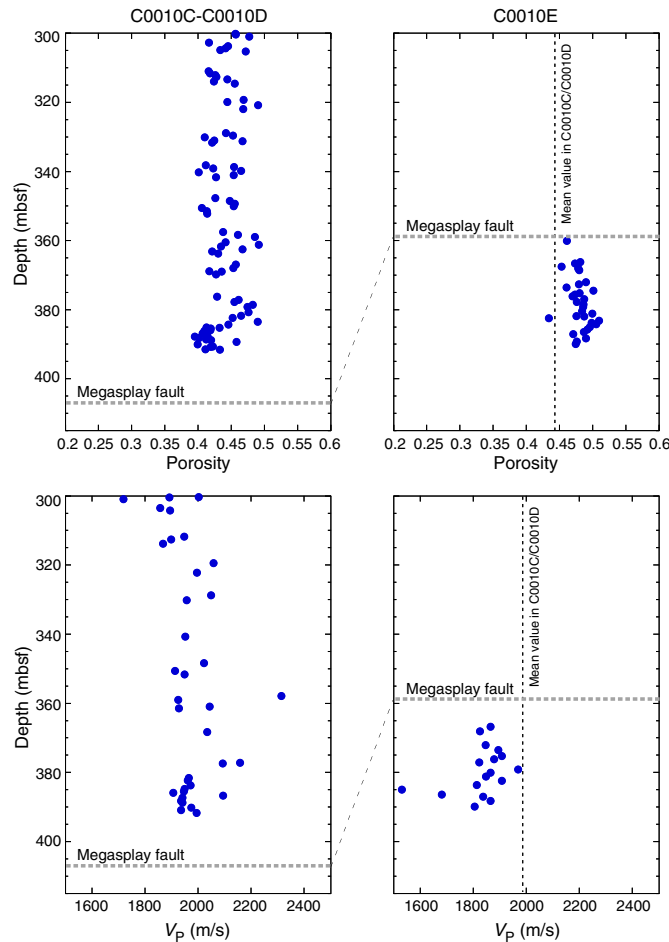
Figure F18. Generalized stratigraphic columns for Holes C0010C and C0010D (hanging wall) and Hole C0010E (footwall).



~350 mbsf. Dips steepen and are up to 50°–60° in the ~50 m above the fault, likely related to deformation caused by slip on the megasplay. Faults and shear zones in the hanging wall also dip moderately. High-angle faults, one of which is identified as a reverse fault, are only observed at ~375 mbsf. Bedding in Hole C0010E in the footwall of the fault is horizontal or gently dipping; unlike the hanging wall, low-angle (<30°) anastomosing shear zones are common in the footwall cores.

Porosity within the hanging wall ranges from 40% to 50% and averages ~42% (Figure F19). Although scattered, there is a distinct increase in porosity in the footwall cored in Hole C0010E, with values ranging from 45% to 50% and averaging 48%. *P*-wave velocity in all orientations increases gradually with depth in the hanging wall in Holes C0010C and C0010D from ~1900 to ~2000 m/s in the interval 300–395 mbsf. In the footwall (Hole C0010E), *P*-wave velocity is nearly constant with depth at ~1880 m/s. Average thermal conductivities are 1.37, 1.47, and 1.3 W/(m·K) for Holes C0010C, C0010D, and C0010E, respectively. In general, thermal conductivity in the hanging wall is higher than in the footwall. The higher *P*-wave velocity and thermal conductivity in the hanging wall relative to the footwall is consistent with its lower porosity.

Figure F19. Porosity and P-wave velocity data, Holes C0010A–C0010E.



Preliminary scientific assessment

Expedition 365 achieved its two primary scientific and operational objectives, including (1) recovery of the GeniusPlug temporary monitoring system with a >5 y record of pressure and temperature conditions within the shallow megasplay fault zone, geochemical samples, and an *in situ* microbial colonization experiment (Figures F8, F9) and (2) installation of a permanent LTBMS with a suite of instruments to monitor seismicity, deformation, and hydrogeological processes. The complex LTBMS sensor array, in combination with the multilevel hole completion, is one of the most ambitious and sophisticated observatory installations in scientific ocean drilling (similar to that in Hole C0002G, deployed in 2010). Additional operational challenges to deployment of the observatory string are presented by the 2500 m water depth and the strong Kuroshio Current (reaching speeds >5 kt during the expedition). Overall, the installation went smoothly, efficiently, and ahead of schedule. The extra time afforded by the efficient observatory deployment was used for coring at Site C0010. Despite challenging hole conditions, the depth interval corresponding to the screened casing across the megasplay fault was successfully sampled in Hole C0010C, and the footwall of the megasplay was sampled in Hole C0010E, with >50% recovery for both zones. Taken together with promising initial results from the GeniusPlug, this represents a clear success in meeting—and exceeding—Expedition 365 objectives.

Notably, many of the previous problems related to running complex observatory arrays in the Kuroshio Current have been successfully mitigated. During deployment “dummy runs” in this area during Expedition 319, VIV of the drill pipe in the water column caused extensive damage to sensors and led to the loss of instruments (Expedition 319 Scientists, 2010). During the most recent NanTroSEIZE LTBMS installation during Expedition 332 (Hole C0002G), VIV was mitigated with the use of ropes attached to the upper portion of the drill pipe, which reduced vibration by disrupting the flow of water around the pipe and prevented the formation of a low-pressure region behind (downstream of) the pipe. However, attachment of ropes, umbilical flatpack, and cables to the pipe still presents an operational challenge and requires considerable time because the lines need to be gathered and strapped to the pipe every ~2 m. During Expedition 365, newly developed moonpool equipment, including a guide roller and completion guide roller, vastly increased efficiency and safety by providing guides to align the umbilical and cables (guide roller) and ropes (completion guide roller) for attachment to the pipe as it was lowered through the moonpool. We attribute much of the operation’s success during the expedition to these advances. The increased efficiency afforded extra days for science operations; as a result, we were able to collect core samples that will provide valuable data to aid in interpretation of the observatory data. The increased efficiency also minimized the time spent suspending sensitive instrumentation in the water column, which in turn minimized the risk of damage due to heave and vibration in the current.

Initial analysis of the GeniusPlug pressure, temperature, chemical, and microbiological experiments has provided promising results. Coring of the thrust wedge immediately above the megasplay fault has yielded key samples for postexpedition analyses and for comparison of pore fluid geochemistry with that sampled by the GeniusPlug. The key outcomes of the expedition include

- Complete recovery of continuous pressure and temperature records from the GeniusPlug, which include high-quality records of formation and seafloor responses to multiple fault slip events, including the 2011 Tohoku M9 earthquake (Figure F11), the 1 April 2016 Mie-Ken Nanto-oki M6 earthquake (Figure F12), and additional tentatively identified slip events associated with VLF earthquakes (one possibly triggered by the Tohoku earthquake and another in October 2015) (Tobin, Hirose, Saffer, Toczko, Maeda, Kubo, and the Expedition 348 Scientists, 2015);
- Recovery of the FLOCS unit and geochemical sampling coils and successful cultivation of microbes from the FLOCS unit (Figure F14);
- Successful deployment of the LTBMS string and completion of the hole (Figure F6); and
- Coring in the deepest part of the thrust wedge above the megasplay fault (Holes C0010C and C0010D) and into the footwall of the fault (Hole C0010E), with >50% recovery of the formation; these samples provide valuable context for formation physical properties and interstitial water geochemistry and will greatly enhance interpretation of the GeniusPlug and LTBMS data sets.

The GeniusPlug record of the Mie-ken Nanto-oki earthquake documents a positive offset in pressure following the event, indicating compressional strain, and is consistent with observations from the previously installed LTBMS in Hole C0002G. This is important because together these data can uniquely distinguish between the two potential focal mechanisms identified by seismological data (a steeply southeast-dipping nodal plane vs. a shallow northwest-dip-

ping one) and provide key evidence supporting a thrusting event either within the accretionary wedge or at the plate interface (Wallace et al., 2016). We anticipate that future analysis of other earthquakes in the pressure record will produce similar insights.

The GeniusPlug chemistry coils provide fluid samples that are, to first order, consistent with interstitial pore fluids collected across the megathrust at nearby Site C0004 (Screaton et al., 2009). However, loss of substantial fluid during recovery (possibly related to gas exsolution and expansion in the coils) in combination with cracking of the membranes for the chemical sampling coils preclude a detailed analysis of the time series data. One reason for the large amount of gas, in particular when compared to earlier FLOCS deployments in oceanic crust, may be the fact that microbial metabolism rates were enhanced in this sedimentary setting with Site C0004 sediment as substrate. Additional targeted analysis of samples and review of the data postexpedition may provide further insights. Care should be taken in future deployments to develop a mechanism to seal the sampling coils and to improve access to the coils on the rig floor to prevent depressurization and/or minimize fluid loss during recovery and transport of the coils to the shipboard laboratories.

The second primary objective of Expedition 365 was to install a permanent LTBMS (Figures F6, F15, F16, F17). This was completed successfully and ahead of schedule. All observatory components were tested at several stages before, during, and after reentry and final deployment. These tests verify that all cables, data transmission, and instruments were not damaged during the deployment procedure and were functioning at the time of cementing and hole completion. After Expedition 365, the LTBMS, including multilevel pressure sensors and the full suite of geodetic and seismological instruments, was connected successfully to DONET during a Japan Agency for Marine-Earth Science and Technology cruise on 19 June 2016. From that time onward, power has been supplied by the cabled network and the data sampling rate for pressure was increased from 60 s to 1 s.

In addition to accomplishing the planned expedition objectives noted above, efficient observatory operations afforded contingency time that was used to core the hanging wall and footwall of the megasplay fault and recover materials representative of the formation where observatory instruments are placed at Site C0010 (Figure F4). The hanging wall is characterized by fractured claystones, whereas the footwall is characterized by less intensely deformed and slightly coarser grained overridden slope apron deposits. These siltstones are similar to those cored at Sites C0001 and C0004 (Figures F18, F19) with some key differences, notably: (1) the hanging wall at Site C0010 has slightly lower porosity and higher P -wave velocity than the hanging wall at Site C0004, consistent with differences in LWD data sets between the two sites and suggesting that the thrust wedge at Site C0010 is slightly more consolidated and/or clay rich than its counterpart along strike; (2) higher calcite content (up to 15 wt%) indicative of deeper environment of deposition closer to the carbonate compensation depth (CCD); and (3) thinner mass transport deposits.

Overall, the expedition was a clear success. All of the scientific and operational goals were achieved and completed well ahead of schedule, allowing for ~5 days of contingency operations that included coring at Site C0010. This is noteworthy because the sites had been logged with LWD during Expedition 319 at the time the casing was emplaced (Expedition 319 Scientists, 2010) but had not yet been cored. Collection of samples will provide key constraints on rock properties and provide valuable context (i.e., pore fluid geo-

chemistry and physical properties) for interpretation of LTBMS and GeniusPlug data. For the earthquake events analyzed in our preliminary review of the data set, the borehole measurements, together with data from the previously installed borehole observatory in Hole C0002G, provide important and unique constraints on both slow earthquakes and the details of rupture in the Mie-ken Nanto-oki earthquake (e.g., Wallace et al., 2016). These examples underscore the essential value of borehole observatories in understanding earthquake and tsunami processes through monitoring in boreholes that place instruments nearby, within, and directly above the earthquake-generating faults.

References

Ando, M., 1975. Source mechanisms and tectonic significance of historical earthquakes along the Nankai Trough, Japan. *Tectonophysics*, 27(2):119–140. [http://dx.doi.org/10.1016/0040-1951\(75\)90102-X](http://dx.doi.org/10.1016/0040-1951(75)90102-X)

Ashi, J., Kuramoto, S., Morita, S., Tsunogai, U., Goto, S., Kojima, S., Okamoto, T., Ishimura, T., Ijiri, A., Toki, T., Kudo, S., Asai, S., and Utsumi, M., 2002. Structure and cold seep of the Nankai accretionary prism off Kumano—outline of the off Kumano survey during YK01-04 Leg 2 cruise. *JAMSTEC Journal of Deep Sea Research*, 20:1–8. (in Japanese, with abstract in English)

Ashi, J., Lallement, S., Masago, H., and the Expedition 315 Scientists, 2009. Expedition 315 summary. In Kinoshita, M., Tobin, H., Ashi, J., Kimura, G., Lallement, S., Screaton, E.J., Curewitz, D., Masago, H., Moe, K.T., and the Expedition 314/315/316 Scientists, *Proceedings of the Integrated Ocean Drilling Program*, 314/315/316: Washington, DC (Integrated Ocean Drilling Program Management International, Inc.). <http://dx.doi.org/10.2204/iodp.proc.314315316.121.2009>

Baba, T., and Cummins, P.R., 2005. Contiguous rupture areas of two Nankai Trough earthquakes revealed by high-resolution tsunami waveform inversion. *Geophysical Research Letters*, 32(8):L08305. <http://dx.doi.org/10.1029/2004GL022320>

Baba, T., Cummins, P.R., and Hori, T., 2005. Compound fault rupture during the 2004 off the Kii Peninsula earthquake (M 7.4) inferred from highly resolved coseismic sea-surface deformation. *Earth, Planets and Space*, 57(3):167–172. <http://www.terrapub.co.jp/journals/EPS/pdf/2005/5703/57030167.pdf>

Baba, T., Cummins, P.R., Hori, T., and Kaneda, Y., 2006. High precision slip distribution of the 1944 Tonankai earthquake inferred from tsunami waveforms: possible slip on a splay fault. *Tectonophysics*, 426(1–2):119–134. <http://dx.doi.org/10.1016/j.tecto.2006.02.015>

Byrne, D.E., Davis, D.M., and Sykes, L.R., 1988. Loci and maximum size of thrust earthquakes and the mechanics of the shallow region of subduction zones. *Tectonics*, 7(4):833–857. <http://dx.doi.org/10.1029/TC007i004p00833>

Expedition 314 Scientists, 2009. Expedition 314 Site C0004. In Kinoshita, M., Tobin, H., Ashi, J., Kimura, G., Lallement, S., Screaton, E.J., Curewitz, D., Masago, H., Moe, K.T., and the Expedition 314/315/316 Scientists, *Proceedings of the Integrated Ocean Drilling Program*, 314/315/316: Washington, DC (Integrated Ocean Drilling Program Management International, Inc.). <http://dx.doi.org/10.2204/iodp.proc.314315316.116.2009>

Expedition 319 Scientists, 2010. Expedition 319 summary. In Saffer, D., McNeill, L., Byrne, T., Araki, E., Toczko, S., Eguchi, N., Takahashi, K., and the Expedition 319 Scientists, *Proceedings of the Integrated Ocean Drilling Program*, 319: Tokyo (Integrated Ocean Drilling Program Management International, Inc.). <http://dx.doi.org/10.2204/iodp.proc.319.101.2010>

Expedition 326 Scientists, 2011. *Expedition 326 Preliminary Report: NanTro-SEIZE Stage 3: Plate Boundary Deep Riser: Top Hole Engineering*. Integrated Ocean Drilling Program. <http://dx.doi.org/10.2204/iodp.pr.326.2011>

Expedition 343/343T Scientists, 2013. Expedition 343/343T summary. In Chester, F.M., Mori, J., Eguchi, N., Toczko, S., and the Expedition 343/343T Scientists, *Proceedings of the Integrated Ocean Drilling Pro-*

gram, 343/343T: Tokyo (Integrated Ocean Drilling Program Management International, Inc.).
<http://dx.doi.org/10.2204/iodp.proc.343343T.101.2013>

Fujiwara, T., Kodaira, S., No, T., Kaiho, Y., Takahashi, N., and Kaneda, Y., 2011. The 2011 Tohoku-Oki earthquake: displacement reaching the trench axis. *Science*, 334(6060):1240. <http://dx.doi.org/10.1126/science.1211554>

Henry, P., Kanamatsu, T., Moe, K., and the Expedition 333 Scientists, 2012. *Proceedings of the Integrated Ocean Drilling Program*, 333: Tokyo (Integrated Ocean Drilling Program Management International, Inc.).
<http://dx.doi.org/10.2204/iodp.proc.333.2012>

Hickman, S., Zoback, M., and Ellsworth, W., 2004. Introduction to special section: preparing for the San Andreas Fault Observatory at depth. *Geophysical Research Letters*, 31(12):L12S01.
<http://dx.doi.org/10.1029/2004GL020688>

Hori, T., Kato, N., Hirahara, K., Baba, T., and Kaneda, Y., 2004. A numerical simulation of earthquake cycles along the Nankai Trough in southwest Japan: lateral variation in frictional property due to the slab geometry controls the nucleation position. *Earth and Planetary Science Letters*, 228(3–4):215–226. <http://dx.doi.org/10.1016/j.epsl.2004.09.033>

Ichinose, G.A., Thio, H.K., Somerville, P.G., Sato, T., and Ishii, T., 2003. Rupture process of the 1944 Tonankai earthquake (M_s 8.1) from the inversion of telesismic and regional seismograms. *Journal of Geophysical Research: Solid Earth*, 108(B10):2497. <http://dx.doi.org/10.1029/2003JB002393>

Ito, Y., Obara, K., Shiomii, K., Sekine, S., and Hirose, H., 2007. Slow earthquakes coincident with episodic tremors and slow slip events. *Science*, 315(5811):503–506. <http://dx.doi.org/10.1126/science.1134454>

Kikuchi, M., Nakamura, M., and Yoshikawa, K., 2003. Source rupture processes of the 1944 Tonankai earthquake and the 1945 Mikawa earthquake derived from low-gain seismograms. *Earth, Planets and Space*, 55(4):159–172. <http://www.terrapub.co.jp/journals/EPS/pdf/2003/5504/55040159.pdf>

Kinoshita, M., Tobin, H., Ashi, J., Kimura, G., Lallemand, S., Screamton, E.J., Curewitz, D., Masago, H., Moe, K.T., and the Expedition 314/315/316 Scientists, 2009. *Proceedings of the Integrated Ocean Drilling Program*, 314/315/316: Washington, DC (Integrated Ocean Drilling Program Management International, Inc.).
<http://dx.doi.org/10.2204/iodp.proc.314315316.2009>

Kopf, A., Araki, E., Toczko, S., and the Expedition 332 Scientists, 2011. *Proceedings of the Integrated Ocean Drilling Program*, 332: Tokyo (Integrated Ocean Drilling Program Management International, Inc.).
<http://dx.doi.org/10.2204/iodp.proc.332.2011>

Kopf, A., Saffer, D., and Toczko, S., 2015. *Expedition 365 Scientific Prospectus: NanTroSEIZE Stage 3: Shallow Megasplay Long-Term Borehole Monitoring System (LTBMS)*. International Ocean Discovery Program.
<http://dx.doi.org/10.14379/iodp.sp.365.2015>

Lay, T., Kanamori, H., Ammon, C.J., Nettles, M., Ward, S.N., Aster, R.C., Beck, S.L., Bilek, S.L., Brudzinski, M.R., Butler, R., DeShon, H.R., Ekström, G., Satake, K., and Sipkin, S., 2005. The great Sumatra-Andaman earthquake of 26 December 2004. *Science*, 308(5725):1127–1133.
<http://dx.doi.org/10.1126/science.1112250>

Ma, K., 2005. Slip zone and energetic of a large earthquake from seismological modeling and fault core of TCDP. *Eos, Transactions American Geophysical Union*, 86(52):T43D-02. (Abstract)
<http://www.agu.org/meetings/fm05/waisfm05.html>

Miyazaki, S., and Heki, K., 2001. Crustal velocity field of southwest Japan: subduction and arc-arc collision. *Journal of Geophysical Research: Solid Earth*, 106(B3):4305–4326. <http://dx.doi.org/10.1029/2000JB900312>

Moore, G.F., Bangs, N.L., Taira, A., Kuramoto, S., Pangborn, E., and Tobin, H.J., 2007. Three-dimensional splay fault geometry and implications for tsunami generation. *Science*, 318(5853):1128–1131.
<http://dx.doi.org/10.1126/science.1147195>

Moore, G.F., Mikada, H., Moore, J.C., Becker, K., and Taira, A., 2005. Legs 190 and 196 synthesis: deformation and fluid flow processes in the Nankai Trough accretionary prism. In Mikada, H., Moore, G.F., Taira, A., Becker, K., Moore, J.C., and Klaus, A. (Eds.), *Proceedings of the Ocean Drilling Program, Scientific Results*, 190/196: College Station, TX (Ocean Drilling Program), 1–25.
<http://dx.doi.org/10.2973/odp.proc.sr.190196.201.2005>

Moore, G.F., Park, J.-O., Bangs, N.L., Gulick, S.P., Tobin, H.J., Nakamura, Y., Sato, S., Tsuji, T., Yoro, T., Tanaka, H., Uraki, S., Kido, Y., Sanada, Y., Kuramoto, S., and Taira, A., 2009. Structural and seismic stratigraphic framework of the NanTroSEIZE Stage 1 transect. In Kinoshita, M., Tobin, H., Ashi, J., Kimura, G., Lallemand, S., Screamton, E.J., Curewitz, D., Masago, H., Moe, K.T., and the Expedition 314/315/316 Scientists, *Proceedings of the Integrated Ocean Drilling Program*, 314/315/316: Washington, DC (Integrated Ocean Drilling Program Management International, Inc.).
<http://dx.doi.org/10.2204/iodp.proc.314315316.102.2009>

Moore, G.F., Taira, A., Klaus, A., Becker, L., Boeckel, B., Cragg, B.A., Dean, A., Fergusson, C.L., Henry, P., Hirano, S., Hisamitsu, T., Hunze, S., Kastner, M., Maltman, A.J., Morgan, J.K., Murakami, Y., Saffer, D.M., Sánchez-Gómez, M., Screamton, E.J., Smith, D.C., Spivack, A.J., Steurer, J., Tobin, H.J., Ujiie, K., Underwood, M.B., and Wilson, M., 2001. New insights into deformation and fluid flow processes in the Nankai Trough accretionary prism: results of Ocean Drilling Program Leg 190. *Geochemistry, Geophysics, Geosystems*, 2(10):1058.
<http://dx.doi.org/10.1029/2001GC000166>

Moore, J.C., and Saffer, D., 2001. Updip limit of the seismogenic zone beneath the accretionary prism of southwest Japan: an effect of diagenetic to low-grade metamorphic processes and increasing effective stress. *Geology*, 29(2):183–186. [http://dx.doi.org/10.1130/0091-7613\(2001\)029<0183:ULOTSZ>2.0.CO;2](http://dx.doi.org/10.1130/0091-7613(2001)029<0183:ULOTSZ>2.0.CO;2)

Moreno, M., Rosenau, M., and Oncken, O., 2010. 2010 Maule earthquake slip correlates with pre-seismic locking of Andean subduction zone. *Nature*, 467(7312):198–202. <http://dx.doi.org/10.1038/nature09349>

Nakanishi, A., Takahashi, N., Park, J.-O., Miura, S., Kodaira, S., Kaneda, Y., Hirata, N., Iwasaki, T., and Nakamura, M., 2002. Crustal structure across the coseismic rupture zone of the 1944 Tonankai earthquake, the central Nankai Trough seismogenic zone. *Journal of Geophysical Research: Solid Earth*, 107(B1). <http://dx.doi.org/10.1029/2001JB000424>

Obana, K., Kodaira, S., Mochizuki, K., and Shinohara, M., 2001. Micro-seismicity around the seaward updip limit of the 1946 Nankai earthquake dislocation area. *Geophysical Research Letters*, 28(12):2333–2336.
<http://dx.doi.org/10.1029/2000GL012794>

Obana, K., Kodaira, S., and Yoshiyuki, K., 2005. Seismicity in the incoming/subducting Philippine Sea plate off the Kii Peninsula, central Nankai Trough. *Journal of Geophysical Research: Solid Earth*, 110(B11):B11311.
<http://dx.doi.org/10.1029/2004JB003487>

Obara, K., and Ito, Y., 2005. Very low frequency earthquakes excited by the 2004 off the Kii Peninsula earthquakes: a dynamic deformation process in the large accretionary prism. *Earth, Planets and Space*, 57(4):321–326.
<http://www.terrapub.co.jp/journals/EPS/pdf/2005/5704/57040321.pdf>

Park, J.-O., Tsuru, T., Kodaira, S., Cummins, P.R., and Kaneda, Y., 2002. Splay fault branching along the Nankai subduction zone. *Science*, 297(5584):1157–1160. <http://dx.doi.org/10.1126/science.1074111>

Ruff, L., and Kanamori, H., 1983. Seismic coupling and uncoupling at subduction zones. *Tectonophysics*, 99(2–4):99–117.
[http://dx.doi.org/10.1016/0040-1951\(83\)90097-5](http://dx.doi.org/10.1016/0040-1951(83)90097-5)

Saffer, D., Kopf, A., Toczko, S., Araki, E., Carr, S., Kimura, T., Kinoshita, C., Kobayashi, R., Machida, Y., Rösner, A., and Wallace, L.M., 2017a. Expedition 365 methods. With contributions by S. Chiyonobu, K. Kanagawa, T. Kanamatsu, G. Kimura, and M.B. Underwood. In Saffer, D., Kopf, A., Toczko, S., and the Expedition 365 Scientists, *NanTroSEIZE Stage 3: Shallow Megasplay Long-Term Borehole Monitoring System*. Proceedings of the International Ocean Discovery Program, 365: College Station, TX (International Ocean Discovery Program).
<http://dx.doi.org/10.14379/iodp.proc.365.102.2017>

Saffer, D., Kopf, A., Toczko, S., Araki, E., Carr, S., Kimura, T., Kinoshita, C., Kobayashi, R., Machida, Y., Rösner, A., and Wallace, L.M., 2017b. Site C0010. With contributions by S. Chiyonobu, K. Kanagawa, T. Kanamatsu, G. Kimura, and M.B. Underwood. In Saffer, D., Kopf, A., Toczko, S., and the Expedition 365 Scientists, *NanTroSEIZE Stage 3: Shallow Megasplay Long-Term Borehole Monitoring System*. Proceedings of the International Ocean Discovery Program, 365: College Station, TX (International Ocean Discovery Program).
<http://dx.doi.org/10.14379/iodp.proc.365.103.2017>

Saffer, D.M., and Marone, C., 2003. Comparison of smectite- and illite-rich gouge frictional properties: application to the updip limit of the seismogenic zone along subduction megathrusts. *Earth and Planetary Science Letters*, 215(1–2):219–235.
[http://dx.doi.org/10.1016/S0012-821X\(03\)00424-2](http://dx.doi.org/10.1016/S0012-821X(03)00424-2)

Schwartz, S.Y., and Rokosky, J.M., 2007. Slow slip events and seismic tremor at circum-Pacific subduction zones. *Reviews of Geophysics*, 45(3):RG3004.
<http://dx.doi.org/10.1029/2006RG000208>

Screaton, E.J., Kimura, G., Curewitz, D., and the Expedition 316 Scientists, 2009. Expedition 316 summary. In Kinoshita, M., Tobin, H., Ashi, J., Kimura, G., Lallemant, S., Screaton, E.J., Curewitz, D., Masago, H., Moe, K.T., and the Expedition 314/315/316 Scientists, *Proceedings of the Integrated Ocean Drilling Program*, 314/315/316: Washington, DC (Integrated Ocean Drilling Program Management International, Inc.).
<http://dx.doi.org/10.2204/iodp.proc.314315316.131.2009>

Seno, T., Stein, S., and Gripp, A.E., 1993. A model for the motion of the Philippine Sea plate consistent with NUVEL-1 and geological data. *Journal of Geophysical Research: Solid Earth*, 98(B10):17941–17948.
<http://dx.doi.org/10.1029/93JB00782>

Simons, M., Minson, S.E., Sladen, A., Ortega, F., Jiang, J., Owen, S.E., Meng, L., Ampuero, J.-P., Wei, S., Chu, R., Helmberger, D.V., Kanamori, H., Hettland, E., Moore, A.W., and Webb, F.H., 2011. The 2011 magnitude 9.0 Tohoku-Oki earthquake: mosaicking the megathrust from seconds to centuries. *Science*, 332(6036):1421–1425.
<http://dx.doi.org/10.1126/science.1206731>

Strasser, M., Dugan, B., Kanagawa, K., Moore, G.F., Toczko, S., Maeda, L., Kido, Y., Moe, K.T., Sanada, Y., Esteban, L., Fabbri, O., Geersen, J., Hammerschmidt, S., Hayashi, H., Heirman, K., Hüpers, A., Jurado Rodriguez, M.J., Kameo, K., Kanamatsu, T., Kitajima, H., Masuda, H., Milliken, K., Mishra, R., Motoyama, I., Olcott, K., Oohashi, K., Pickering, K.T., Ramirez, S.G., Rashid, H., Sawyer, D., Schleicher, A., Shan, Y., Skarbek, R., Song, I., Takeshita, T., Toki, T., Tudge, J., Webb, S., Wilson, D.J., Wu, H.-Y., and Yamaguchi, A., 2014. Expedition 338 summary. In Strasser, M., Dugan, B., Kanagawa, K., Moore, G.F., Toczko, S., Maeda, L., and the Expedition 338 Scientists, *Proceedings of the Integrated Ocean Drilling Program*, 338: Yokohama, Japan (Integrated Ocean Drilling Program).
<http://dx.doi.org/10.2204/iodp.proc.338.101.2014>

Tanioka, Y., and Satake, K., 2001. Detailed coseismic slip distribution of the 1944 Tonankai earthquake estimated from tsunami waveforms. *Geophysical Research Letters*, 28(6):1075–1078.
<http://dx.doi.org/10.1029/2000GL012284>

Tobin, H., Hirose, T., Saffer, D., Toczko, S., Maeda, L., Kubo, Y., and the Expedition 348 Scientists, 2015. *Proceedings of the Integrated Ocean Drilling Program*, 348: College Station, TX (Integrated Ocean Drilling Program).
<http://dx.doi.org/10.2204/iodp.proc.348.2015>

Tobin, H.J., and Kinoshita, M., 2006a. *NanTroSEIZE Project Stage 1 Scientific Prospectus: Investigations of Seismogenesis at the Nankai Trough, Japan*. Integrated Ocean Drilling Program.
<http://dx.doi.org/10.2204/iodp.sp.nantrorseize1.2006>

Tobin, H.J., and Kinoshita, M., 2006b. NanTroSEIZE: the IODP Nankai Trough Seismogenic Zone Experiment. *Scientific Drilling*, 2:23–27.
<http://dx.doi.org/10.2204/iodp.sd.2.06.2006>

Underwood, M.B., Saito, S., Kubo, Y., and the Expedition 322 Scientists, 2010. Expedition 322 summary. In Saito, S., Underwood, M.B., Kubo, Y., and the Expedition 322 Scientists, *Proceedings of the Integrated Ocean Drilling Program*, 322: Tokyo (Integrated Ocean Drilling Program Management International, Inc.).
<http://dx.doi.org/10.2204/iodp.proc.322.101.2010>

Wallace, L.M., Araki, E., Saffer, D., Wang, X., Roesner, A., Kopf, A., Nakanishi, A., Power, W., Kobayashi, R., Kinoshita, C., Toczko, S., Kimura, T., Machida, Y., and Carr, S., 2016. Near-field observations of an offshore M_w 6.0 earthquake from an integrated seafloor and subseafloor monitoring network at the Nankai Trough, southwest Japan. *Journal of Geophysical Research: Solid Earth*, 121(11):8338–8351.
<http://dx.doi.org/10.1002/2016JB013417>

Wang, K., and Hu, Y., 2006. Accretionary prisms in subduction earthquake cycles: the theory of dynamic Coulomb wedge. *Journal of Geophysical Research: Solid Earth*, 111(B6):B06410.
<http://dx.doi.org/10.1029/2005JB004094>

Yamano, M., Kinoshita, M., Goto, S., and Matsubayashi, O., 2003. Extremely high heat flow anomaly in the middle part of the Nankai Trough. *Physics and Chemistry of the Earth*, 28(9–11):487–497.
[http://dx.doi.org/10.1016/S1474-7065\(03\)00068-8](http://dx.doi.org/10.1016/S1474-7065(03)00068-8)